7 QCD Comparisons

Quantum Chromodynamics (QCD) is the field theory that describes the strong interactions. In this analysis, QCD is examined in two different ways. First, the structure functions shown in Chapter 6 are used to test the theory of perturbative QCD. The theory actually makes no predictions about the structure functions themselves, but predicts the change in the slope of the structure functions versus Q^2, which in turn depends on the QCD scale parameter $\Lambda_{\overline{\mathrm{MS}}}$. To test the validity of the theory, the perturbative QCD predictions are compared against the slope of the structure functions incorporating both the statistical and systematic errors.

The second way QCD is applied in this analysis is to assume that the theory is correct and incorporate the experimental systematic errors in the QCD fit. This yields a precise measurement of $\Lambda_{\overline{\mathrm{MS}}}$ and $\alpha_S(M_Z^2)$, the coupling strength of the strong interaction. Since the structure functions and the systematic errors are being interpreted in the context of a model of QCD, it is important to specify the exact model used. This is done in the following Section.

In general, two different types of QCD fits are performed:

- The xF_3-only fit (or non-singlet fit). The QCD model is used to predict the evolution of xF_3 versus Q^2 (see Section 1.2.4.3). The advantage of this fit is that the evolution equation for xF_3 (see Equation 7.12) does not involve the gluon distribution, which cannot be directly measured by this experiment. This approach to determining $\Lambda_{\overline{\mathrm{MS}}}$ is unique to a neutrino experiment, since the other available techniques all involve making some assumptions about the gluons.

- The F_2 and xF_3 fit (combined singlet and non-singlet fit). The QCD model is used to simultaneously predict the evolution of F_2 and xF_3 versus Q^2. Although this method requires some parameterization of the gluon distribution in the QCD fit, it has the advantage of including all the structure-function data. The result of this increase in statistics is that the statistical and systematic errors on $\Lambda_{\overline{\rm MS}}$ are substantially reduced compared to the xF_3-only fit. In addition, this fit gives information on the shape and size of the gluon distribution.

7.1 The QCD Model

The procedure used to implement the theory of QCD is based on a computer program originally written by Dennis Duke and Jeff Owens [Dev83]. The χ^2 minimization was performed by using the function-minimization program MINUIT [Jam94]. After the Duke and Owens program was given to the CCFR collaboration, it was modified by Ed Oltman [Olt89] and William Seligman to suit the needs of the present analysis. Some of these changes were:

- performing a polynomial interpolation on the (*x*,*s*) grid (see Section 7.1.3; formerly the interpolation was linear);

- obtaining theoretical predictions for $2xF_1$, xF_3^{ν}, and $xF_3^{\overline{\nu}}$, in addition to the values of F_2^{ν}, F_2^{ℓ}, and $\left\langle xF_3 \right\rangle$ that the program originally provided;

- testing alternative parameterizations for the parton distributions (see Section 7.2.1);

- modifying the χ^2 calculation for the global systematic error analysis (see Section 7.3).

The following sub-sections describe the overall operation of the program. The FORTRAN source code for the QCD evolution is included in Appendix C.

7.1.1 Initial Parton Distributions

The QCD model starts with parameterizations of the parton distributions at a given Q_0^2. For this analysis, the typical value assigned is $Q_0^2 = 5 GeV^2$, which according to Ref. [Dev83] is the lower limit of the validity of the target mass correction (see Section 7.1.5).

For the xF_3-only fit, only the non-singlet quark distribution, q_{NS}, need be specified:

$$xq_{NS}(x,Q_0^2) = A_{NS} x^{\eta_1} (1-x)^{\eta_2} \tag{7.1}$$

The parameters in Equation 7.1, namely η_1, η_2, and A_{NS}, are variables whose values are determined by the MINUIT χ^2 minimization.

For the F_2 and xF_3 fit, two additional parton distributions are needed: the singlet quark distribution and the gluon distribution, q_S and G. These are parameterized by

$$xq_S(x,Q_0^2) = xq_{NS}(x,Q_0^2) + A_S (1-x)^{\eta_S} \tag{7.2}$$

$$xG(x,Q_0^2) = A_G (1-x)^{\eta_G} \tag{7.3}$$

which leads to additional parameters included in the fit: A_S, η_S, A_G, and η_G. The functional forms for q_{NS}, q_S, and G come from theoretical predictions on the behavior of the parton distributions at small and large x [Rob90].

The remaining parameter to be varied by MINUIT, $\Lambda_{\overline{\mathrm{MS}}}$, enters into the fit via the evolution equations (see section 7.1.3). It affects these equations via the value of $\alpha_S(Q^2)$, which is determined in next-to-leading-order from

$$\ln\left(\frac{Q^2}{\Lambda^2_{\overline{\mathrm{MS}}}}\right) = \frac{4\pi}{\beta_0 \alpha_S\left(Q^2\right)} - \frac{\beta_1}{\beta_0^2}\ln\left[\frac{4\pi}{\beta_0 \alpha_S\left(Q^2\right)} + \frac{\beta_1}{\beta_0^2}\right] \tag{7.4}$$

with

$$\beta_0 = 11 - \frac{2}{3}N_f \tag{7.5}$$

and

$$\beta_1 = 102 - \frac{38}{3}N_f \tag{7.6}$$

where N_f = number of quark flavors. In these QCD fits, N_f was allowed to vary as a function of Q^2, with thresholds set at $N_f = 3$ for $Q^2 < (1.5\,GeV)^2$, $N_f = 4$ for $(1.5\,GeV)^2 < Q^2 < (4.5\,GeV)^2$, and $N_f = 5$ for $Q^2 > (4.5\,GeV)^2$. For this analysis, the value of $\Lambda_{\overline{\mathrm{MS}}}$ is always the value for 4 quark flavors, denoted by $\Lambda^{(4)}_{\overline{\mathrm{MS}}}$, which was chosen to simplify comparison of this result from those of previous deep-inelastic scattering experiments. The mean Q^2 of the data used in the QCD fit is 30 GeV^2, just above the threshold of *b*-quark production.

7.1.2 Comments on Parton Sum Rules

In previous QCD analyses performed by this collaboration [Olt89, Leu91, Qui92] the parameters A_{NS} and A_G were not fit parameters, but were constrained by the "Fermion

Conservation Rule" and the "Momentum Sum Rule" respectively. This section describes the reasons why these sum-rule constraints were removed for the present analysis.

7.1.2.1 The Fermion Conservation Rule

The Fermion Conservation Rule sets the number of valence quarks in the proton to 3:

$$\int_0^1 \frac{xq_{NS}}{x} dx = 3 \tag{7.7}$$

However, when this constraint was imposed on the non-singlet parameterization of Equation 7.1, the χ^2 of the fit was poor. In an attempt to improve the quality of the fit, alternate parameterizations were explored. The parameterization selected for the analysis reported in Ref. [Qui93] was

$$xq_{NS}(x,Q_0^2) = A_{NS} x^{\eta_1} (1-x)^{\eta_2} + B_{NS} x^{\eta_3} \tag{7.8}$$

With this parameterization, and with the constraint given in Equation 7.7, the value of A_{NS} is determined analytically by

$$A_{NS} = \frac{3 - \left(B_{NS} / \eta_3 \right)}{\beta\left(\eta_1, \eta_2 + 1 \right)} \tag{7.9}$$

While the resulting fit had a good χ^2, the values of the parameters were odd: B_{NS} would be quite small (10^{-4} or less), too small to affect the shape of the parton distribution or the Q^2 evolution, but the value of B_{NS} / η_3 would be substantial (~ 0.3). The reason for this behavior is that the addition of the B_{NS} / η_3 term in Equation 7.9 allowed MINUIT to violate the Fermion Conservation Rule of Equation 7.7, without affecting the shape of the parton distribution themselves.

The question now is: why does the QCD fit not agree with the Fermion Conservation Rule? For the answer, it must be recalled that this constraint is related to the Gross-Llewellyn-Smith Sum Rule (GLS Sum Rule) constraint in QCD [Har95]:

$$\underbrace{\int_0^1 dx \frac{xq_{NS}}{x} = 3}_{\substack{\text{Fermion Conservation Rule (parton model)}}} \xrightarrow[\text{QCD}]{}$$

$$\underbrace{\int_0^1 dx \frac{xF_3}{x}}_{\substack{\text{GLS Sum Rule (measured)}}} = 3\left(\underbrace{1 - \frac{\alpha_s}{\pi}}_{\substack{\text{In D\&O program}}} - a\left(n_f\right)\left(\frac{\alpha_s}{\pi}\right)^2 - b\left(n_f\right)\left(\frac{\alpha_s}{\pi}\right)^3 - HO \right) - \Delta HT \tag{7.10}$$

where "*HO*" refers to higher-order terms in α_S, and "*HT*" refers to higher-twist terms. In the Duke and Owens program, the splitting functions and coefficient functions of Equations 7.12-7.20 are calculated only to next-to-leading-order (NLO) in α_s. The values of the NNLO and NNNLO coefficients for the GLS Sum Rule, $a\left(n_f\right)$ and $b\left(n_f\right)$, have been calculated. The higher-order calculable contributions subtract about 15% from the GLS Sum Rule at the Q_0^2 of this analysis [Har95]. Hence the Duke and Owens' program's apparent "violation" of the Fermion Conservation rule is most likely related to the higher-order corrections that are needed at low Q^2.

The need to remove the constraint of the Fermion Conservation Rule from the QCD analysis has two implications:

- The value of $\Lambda_{\overline{\text{MS}}}$ from this analysis is determined from a NLO QCD fit. When converting $\Lambda_{\overline{\text{MS}}}^{\text{NLO}}$ to $\alpha_S(Q^2)$, only the NLO expression of Equation 7.4 should be used.

- Although the NNLO and NNNLO splitting functions and hard-scattering coefficients are not yet available, the corresponding corrections to the GLS Sum Rule are. It should therefore be possible to independently determine $\alpha_S(Q^2)$ to NNNLO from this data by fitting the measured $\int dx\, xF_3/x$ to the form of Equation 7.10. Deborah Harris and Columbia student John Kim are preparing this analysis from the data presented in this thesis.

Another reason for difficulties in applying the Fermion Conservation Rule to a fit involving the CCFR data is the possible nuclear dependence of $\int dx\, xF_3/x$. However, theoretical predictions [Sid95] indicate that this effect should be less than 1% over the (x, Q^2) range of this data.

7.1.2.2 The Momentum Sum Rule

The Momentum Sum Rule states that the total momentum of the proton is carried by the quarks and the gluons:

$$\int_0^1 \left(xq_S(x, Q_0^2) + xG(x, Q_0^2) \right) dx = 1 \tag{7.11}$$

In the analyses of Refs. [Olt89, Leu91, Qui92], the Momentum Sum Rule was used to constrain the value of A_G.

Given the parameterizations of xq_S and xG shown in Equations 7.2 and 7.3, the values of the distributions at low *x* contribute the dominant part of this integral. However, the cut of $Q^2 > 5$ applied in the QCD fit implies an effective *x* cut in our data; Figures 6.19 and 6.21 illustrate this. The low-*x* data that would form the major constraint on the integral of Equation 7.11 is not included in the fit, and so the value of the Momentum Sum Rule

would depend mostly on the parameterizations chosen for q_S and G. Hence, the Momentum Sum Rule was removed as a constraint in the QCD fit.

It should be noted that this decision was based solely on the basis of maintaining the rigor of the analysis. The presence or absence of the Momentum Sum Rule constraint has a small effect on the QCD fit: removing the constraint reduces Λ by 15 *MeV* and reduces the χ^2 by 3 units for 164 degrees of freedom.

7.1.3 Evolution Equations

Given a set of parton distributions parameterized at Q_0^2, QCD predicts the parton distributions at any other Q^2. The evolution equations (1.81-1.83) are implemented in the Duke and Owens program by:

$$\frac{dq^{NS}(x,s)}{ds} = t\frac{\alpha_S(t)}{2\pi}\int_x^1 \frac{dy}{y} q^{NS}(y,s)\, P_{qq}\left(\frac{x}{y}\right) \tag{7.12}$$

$$\frac{dq^{S}(x,s)}{ds} = t\frac{\alpha_S(s)}{2\pi}\int_x^1 \frac{dy}{y}\left[q^{S}(y,s)\, P_{qq}^{S}\left(\frac{x}{y}\right) + G(y,s)\, P_{qG}\left(\frac{x}{y}\right)\right] \tag{7.13}$$

$$\frac{dG(x,s)}{ds} = t\frac{\alpha_S(s)}{2\pi}\int_x^1 \frac{dy}{y}\left[q^{S}(y,s)\, P_{Gq}\left(\frac{x}{y}\right) + G(y,s)\, P_{GG}\left(\frac{x}{y}\right)\right] \tag{7.14}$$

where

$$t = \ln\left(Q^2/\Lambda^2\right) \tag{7.15}$$

$$s = \ln\left[\ln\left(Q^2/\Lambda^2\right)\Big/\ln\left(Q_0^2/\Lambda^2\right)\right] = \ln\left(t/t_0\right) \tag{7.16}$$

$$q^{NS}(x,Q^2) = \sum_i \left(q^i - \bar{q}^i \right) = u_V + d_V \tag{7.17}$$

$$q^{S}(x,Q^2) = \sum_i \left(q^i + \bar{q}^i \right) \tag{7.18}$$

$G(x,Q^2)$ is the gluon distribution, and the P's are the splitting functions described in Section 1.2.4.3. The NLO splitting functions in the $\overline{\text{MS}}$ scheme are given in Refs. [Flo81, Her80].

Given the parton distributions of Equations 7.1-7.3, the QCD-evolution calculation proceeds as follows:

- Evaluate the slopes $\partial q(x,s)/\partial s$ from the right-hand side of Equation 7.12 (for an xF_3-only fit) or all three equations 7.12-7.14 (for a combined F_2 and xF_3 fit) at $Q^2 = Q_0^2$ (i.e., $s = 0$).

- Given the slopes $\partial q(x,s)/\partial s$ determined in the previous step, compute $q(x,s+\partial s)$ using a predictor-corrector method; also compute $G(x,s+\partial s)$ for combined fits.

- Let $s' = s + \partial s$. Compute the right-hand sides of Equations 7.12-7.14 for $q(x,s')$ and $G(x,s')$.

- Repeat the previous two steps until the entire Q^2 range of the experiment has been spanned in s.

The parton distributions q^{NS}, q^{S}, and G, are computed at discrete values of x and s and are stored in the program as a grid in (x_i, s_i). When the program requires a parton distribution at an arbitrary value of (x,s), it is obtained from the grid via a linear interpolation in s and a polynomial interpolation in x.

7.1.4 Hard-Scattering Integrals

To convert the parton distributions to the physically-measured structure functions, the hard-scattering integrals must be computed (see Section 1.2.4.4):

$$F_3(x,Q^2) = \int_x^1 dy \left[C_3^q\left(\frac{x}{y},Q^2\right) q^{NS}(x,Q^2) \right] \tag{7.19}$$

$$x^{-1}F_2(x,Q^2) = \int_x^1 dy \left[C_2^q\left(\frac{x}{y},Q^2\right) q^{S}(x,Q^2) + C_2^G\left(\frac{x}{y},Q^2\right) G(x,Q^2) \right] \tag{7.20}$$

The formulae for the hard-scattering coefficient functions C_i to NLO in the $\overline{\text{MS}}$ scheme are given in Ref. [Her80].

7.1.5 Target Mass Correction

In the derivation of the structure-function formalism in Section 1.2.2, the target and constituent quark masses were ignored in deriving the Q^2-dependence of the structure functions. In the non-perturbative regime of large *x* and small Q^2, the assumption of zero target mass is no longer valid. The target mass correction [Geo76] gives the correction of the structure-functions in Equation 1.27 relative to the observed structure functions. These corrections are:

$$F_2^{TMC} = \frac{x^2}{k^2}\frac{F_2^{QCD}(\xi,Q^2)}{\xi^2} + \frac{6M^2}{Q^2}\frac{x^3}{k^4}I_1 + \frac{12M^4}{Q^4}\frac{x^4}{k^5}I_2 \tag{7.21}$$

$$xF_3^{TMC} = \frac{x^2}{k^2}\frac{xF_3^{QCD}(\xi,Q^2)}{\xi^2} + \frac{2M^2}{Q^2}\frac{x^3}{k^3}I_3 \tag{7.22}$$

where

$$k = \left(1 + \frac{4x^2 M^2}{Q^2}\right)^{\frac{1}{2}} \tag{7.23}$$

$$\xi = \frac{2x}{1+k} \tag{7.24}$$

$$I_1 = \int_\xi^1 du \frac{F_2^{QCD}(u, Q^2)}{u^2} \tag{7.25}$$

$$I_2 = \int_\xi^1 du \int_u^1 dv \frac{F_2^{QCD}(v, Q^2)}{v^2} \tag{7.26}$$

$$I_3 = \int_\xi^1 du \frac{xF_3^{QCD}(u, Q^2)}{u^2} \tag{7.27}$$

7.1.6 Higher-Twist Effects

As the nucleon structure is probed to values below $Q^2 \sim 5\ GeV^2$, perturbative QCD begins to fail. The deviation of the observed structure-function evolution from the predicted evolution of Equations 7.12-7.14 is expressed in terms involving powers of $1/Q^2$. These terms are collectively known as "higher-twist" effects (HT). Some higher-twist effects have been calculated (e.g.; the target mass correction described in the previous Section), but a complete calculation of all higher-twist effects to all powers of Q^2 is not yet available. The higher-twist correction is expressed as

$$F^{\text{Measured}} = F^{\text{Perturbative QCD Prediction}} \left(1 + \frac{D_2(x)}{Q^2} + \frac{D_4(x)}{Q^4} + \ldots\right) \tag{7.28}$$

where $F = F_2$ or xF_3.

A measurement of the higher-twist effects in F_2 was performed using the combined electron scattering data at SLAC and the muon scattering data from BCDMS [Vir92]. In the referenced paper, the QCD prediction of $F_2^{\ell D}$ with the target mass effects applied was compared against the SLAC/BCDMS measurements; the deviation was attributed to the higher-twist effects. Similar analyses have been performed on neutrino deep-inelastic scattering data by Sidorov. One analysis was based on the previous CCFR analysis of data from E744 and E770 [Sid96a], and the other was based on all other neutrino scattering data available apart from CCFR [Sid96b]. As might be expected, the effects were most important in the region of high *x* and low Q^2, in the kinematic region where perturbative QCD is expected to fail.

Recently, a renormalon-based theoretical calculation of the higher-twist effects has become available [Das96, Dok95]; since the authors of the first referenced paper are Dasgupta and Webber, this collaboration denotes the calculation as the "D&W calculation." Figures 7.1 and 7.2 display the results of the D&W calculation for D_2 and D_4, along the F_2 higher-twist measurement from Ref. [Vir92]. Figure 7.3 displays the result of the D&W calculation for the xF_3 D_2 term only, along the with the NLO results from Refs. [Sid96a, Sid96b].

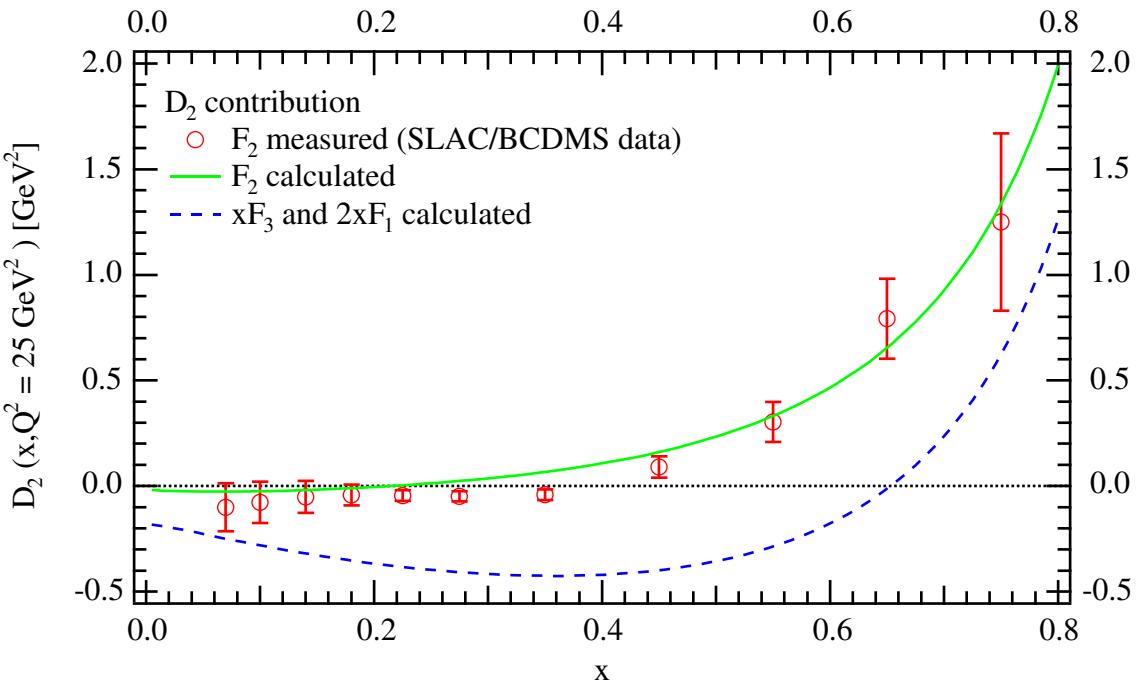

Figure 7.1: D_2 higher-twist term as calculated in Refs. [Das96, Dok95]. The measurement of the F_2 D_2 term from Ref. [Vir92] is included.

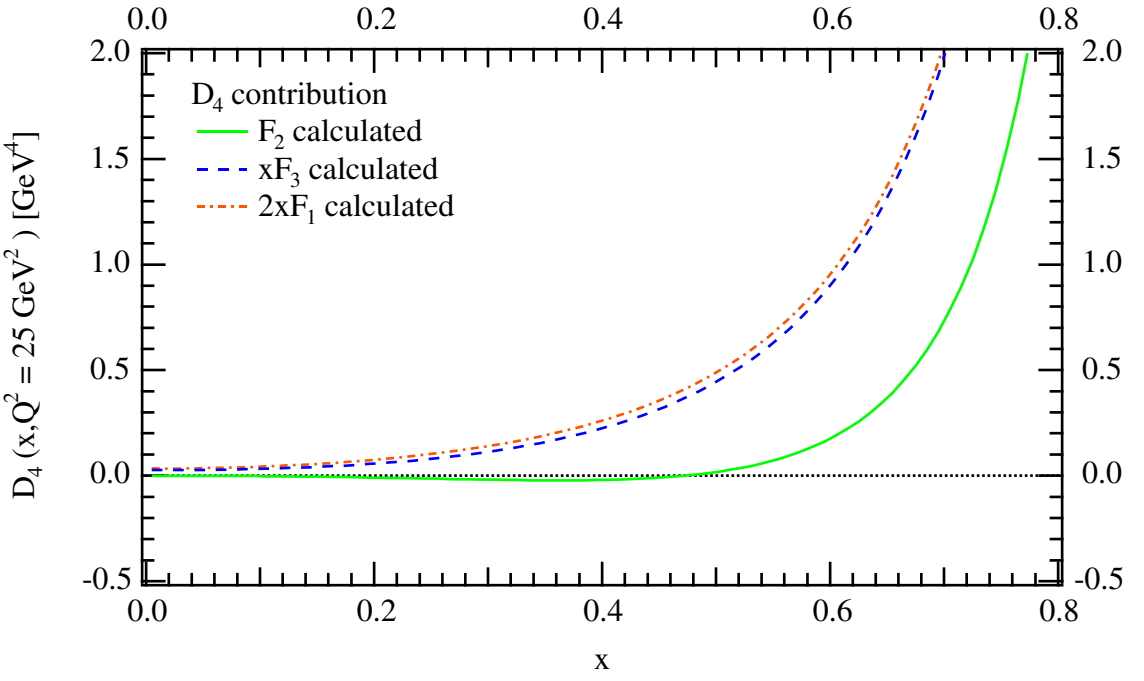

Figure 7.2: D_4 higher-twist term as calculated in Refs. [Das96, Dok95]. Bryan Webber is thanked for the program that generated these two Figures.

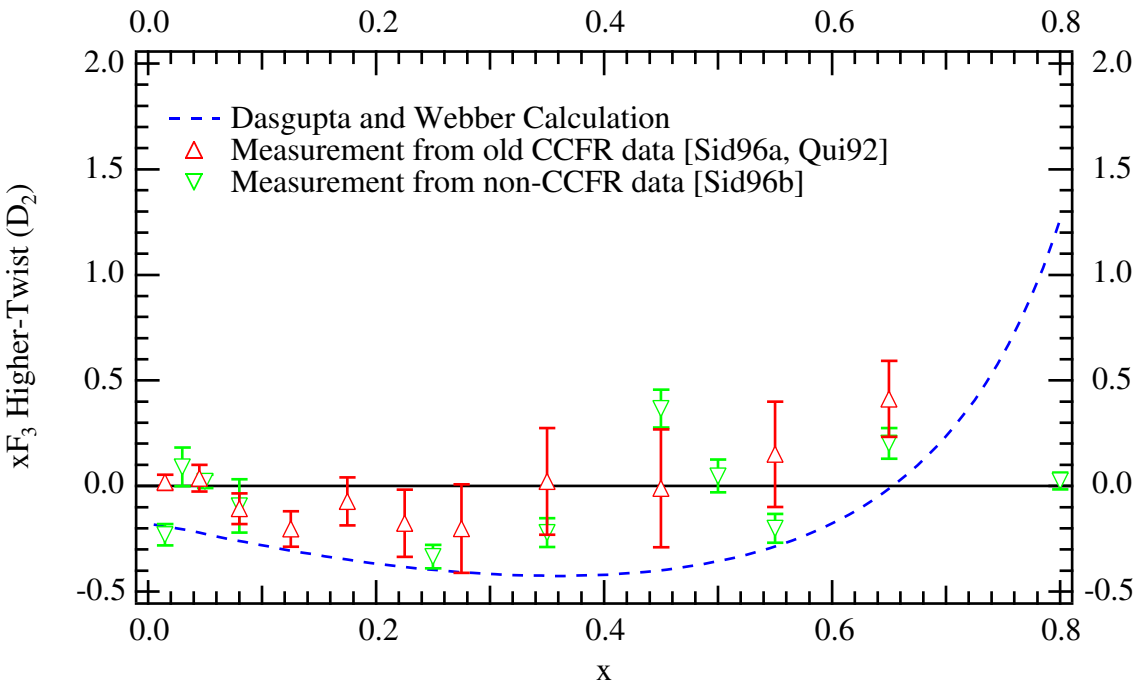

Figure 7.3: xF_3 D_2 higher-twist term as calculated in Refs. [Das96, Dok95]. The measurement of the xF_3 D_2 term from Refs. [Sid96a, Sid96b] is included.

The measurement of the xF_3 D_2 term in Figure 7.3 displays a smaller value for the higher-twist term than the D&W calculation, and this measurement is based in part on the previous CCFR data which is superseded by the present analysis. While the values of the D&W calculation agree with the F_2 D_2 measurement, the measurement was made assuming a value of $\alpha_S(M_Z^2) = 0.113$ which is lower than the present CCFR analysis indicates (see below); this would tend to increase the measured value of the higher-twist term.

Given the above uncertainties in the measurement and calculation of the higher-twist terms, this analysis makes a conservative estimate of the error due to higher-twist effects. The central value of the higher-twist applied to the QCD fit was taken to be

$$F^{\text{Theory}} = F^{\text{Perturbative QCD Prediction}}\left(1+\frac{S\times D_2^{DW}(x)}{Q^2}+\frac{S\times D_4^{DW}(x)}{Q^4}\right) \tag{7.29}$$

where $D_2^{DW}(x)$ and $D_4^{DW}(x)$ are the values from the D&W calculation, and $S = 0.5$. The systematic error is obtained by repeating the QCD fit with $S = 0$ (that is, no higher-twist correction) and $S = 1$ (that is, using the full value from the D&W calculation). The result is that the systematic error due to higher-twist is 17 *MeV* for the xF_3-only fit, and 13 *MeV* for the combined F_2 and xF_3 fit.

7.1.7 Forming the χ^2

The previous sections described how the program calculates xF_3^{theory} and F_2^{theory}. The χ^2 calculation that compares the data with the theory in the combined F_2 and xF_3 fit must incorporate the statistical errors ΔF_2, ΔxF_3, and $\Delta F_2 \Delta xF_3$. Defining the structure-function vector as

$$\vec{\mathbf{F}} = \begin{pmatrix} F_2(x,Q^2) \\ xF_3(x,Q^2) \end{pmatrix} \tag{7.30}$$

and the structure-function error matrix

$$\hat{\mathbf{V}} = \begin{pmatrix} (\Delta F_2)^2 & \Delta F_2 \Delta xF_3 \\ \Delta F_2 \Delta xF_3 & (\Delta xF_3)^2 \end{pmatrix} \tag{7.31}$$

Then the χ^2 is calculated by summing over all the (x,Q^2) bins that pass the cuts:

$$\chi^2 = \sum_{(x,Q^2)\text{bins}} \left[\left(\vec{\mathbf{F}}^{data} - \vec{\mathbf{F}}^{theory}\right)^{\mathrm{T}} \hat{\mathbf{V}}^{-1} \left(\vec{\mathbf{F}}^{data} - \vec{\mathbf{F}}^{theory}\right)\right] \tag{7.32}$$

$$= \sum_{(x,Q^2)\text{bins}} \begin{bmatrix} \left(F_2^{theory} - F_2^{data}\right)^2 v_{22} \\ + \left(xF_3^{theory} - xF_3^{data}\right)^2 v_{33} \\ +2\left(F_2^{theory} - F_2^{data}\right)\left(xF_3^{theory} - xF_3^{data}\right) v_{23} \end{bmatrix} \tag{7.33}$$

where

$$\hat{\mathbf{V}}^{-1} = \begin{bmatrix} v_{22} & v_{32} \\ v_{23} & v_{33} \end{bmatrix} = \frac{1}{\det \hat{\mathbf{V}}} \begin{bmatrix} \left(\Delta xF_3\right)^2 & -\Delta F_2 \Delta xF_3 \\ -\Delta F_2 \Delta xF_3 & \left(\Delta F_2\right)^2 \end{bmatrix} \tag{7.34}$$

and $v_{23} = v_{32}$. As a check, it can be noted that if $\Delta F_2 \Delta xF_3 = 0$, Equation 7.32 becomes (independently for F_2 and xF_3) $\chi^2 = \sum_{(x,Q^2)\text{bins}} \left(f^{data} - f^{theory}\right)^2 \Big/ \Delta f^2$, the familiar expression for calculating a χ^2.

7.2 Tests of QCD

7.2.1 Fit Results

As described above, the parameters $\Lambda_{\overline{\text{MS}}}$, η_1, η_2, A_{NS} and, for combined F_2 and xF_3 fits, A_S, η_S, A_G, η_G, are varied by MINUIT to minimize the χ^2 between NLO QCD and the data. The following cuts are applied to the structure-function data:

- $Q^2 > 5 GeV^2$ and $W^2 > 10 GeV^2$ – to eliminate the non-perturbative region [Bel88, Bel92], and to minimize the effects of any higher-twist corrections to the QCD fit (see Section 7.1.6).

- $x < 0.7$ – to eliminate the region with large Fermi-motion and Monte-Carlo corrections (see Section 6.1.3).

- The relative statistical error (both $\Delta xF_3 / xF_3$ and $\Delta F_2 / F_2$) must be less than 0.5. This cut was chosen to eliminate bins with poor statistics.

The results of the fits are given in Table 7.1; Tables 7.2 and 7.3 give the error matrix and correlation matrix for the xF_3-only fit; Table 7.4 and 7.5 give the error matrix and correlation matrix for the combined F_2 and xF_3 fit. Figures 6.19 through 6.22 show the results of the QCD fit graphically, in *x* bins as a function of Q^2; Figures 7.4 and 7.5 show the same fit in Q^2 bins as a function of *x*.

The statistical error on $\Lambda_{\overline{\text{MS}}}$ from the combined F_2 and xF_3 fit is roughly half that of the xF_3-only fit; this is the result of including the additional F_2 data in the fit. Even though the values of $F_2 \approx xF_3$ for $x > 0.5$ (see Section 6.5), the statistical error on F_2 is smaller, and hence the statistical error on $\Lambda_{\overline{\text{MS}}}$ is smaller, because xF_3 is determined by the *difference* between the number of neutrino and anti-neutrino events, but F_2 is determined by the *sum* of neutrino and anti-neutrino events.

The χ^2/DOF from the combined fit indicates a lower probability than that from the xF_3 fit. The increase in χ^2 is uniformly distributed over the kinematic region of the fit. This increase is caused by the smaller F_2 statistical errors, which make the χ^2 of the fit more sensitive to systematic effects. The global systematic fits described in the next section deal with the effects of the systematic errors on the χ^2 and greatly improve the quality of the fit.

Table 7.1: Results of QCD fits to the structure functions. "Prob" is the integrated upper tail of the χ^2 distribution for the given number of degrees of freedom (DOF). "FSR" is the value of the left-hand side of the integral in the Fermion Sum Rule in Equation 7.7. "MSR" is the value of the left-hand side of the integral of the Momentum Sum Rule in Equation 7.11.

Number		xF_3-only fit	F_2 and xF_3 fit
1	$\Lambda_{\overline{\text{MS}}}$ [MeV]	387 ± 42	381 ± 24
2	η_1	0.801 ± 0.010	0.804 ± 0.008
3	η_2	3.88 ± 0.03	3.91 ± 0.02
4	A_{NS}	8.57 ± 0.20	8.65 ± 0.16
5	A_S		1.52 ± 0.02
6	η_S		7.82 ± 0.09
7	A_G		1.94 ± 0.24
8	η_G		4.44 ± 0.65
	χ^2 / DOF	81.4 / 82	190.6 / 164
	Prob	50%	8%
	FSR	2.84	2.85
	MSR		0.93

Table 7.2: Error matrix σ_{ij} from the xF_3-only fit. The parameter numbers are defined in Table 7.1.

Number	1	2	3	4
1	0.152E-02	0.102E-04	0.654E-03	-0.167E-02
2	0.102E-04	0.941E-04	0.224E-03	0.180E-02
3	0.654E-03	0.224E-03	0.931E-03	0.393E-02
4	-0.167E-02	0.180E-02	0.393E-02	0.385E-01

Table 7.3: Correlation coefficients $\left(\sigma_{ij}\right)\Big/\left(\sigma_{ii}\sigma_{jj}\right)^{1/2}$ from the xF_3-only fit. The parameter numbers are defined in Table 7.1.

Number	GLOBAL	1	2	3	4
1	0.97748	1.000	0.027	0.550	-0.218
2	0.98502	0.027	1.000	0.757	0.946
3	0.97957	0.550	0.757	1.000	0.657
4	0.99372	-0.218	0.946	0.657	1.000

Table 7.4: Error matrix σ_{ij} from the combined F_2 and xF_3 fit. The parameter numbers are defined in Table 7.3.

#	1	2	3	4	5	6	7	8
1	0.484E-03	0.963E-06	-0.160E-03	0.670E-03	-0.125E-03	0.458E-03	-0.341E-02	-0.866E-02
2	0.963E-06	0.698E-04	0.145E-03	0.131E-02	0.993E-04	0.405E-03	-0.767E-04	-0.331E-03
3	-0.160E-03	0.145E-03	0.420E-03	0.276E-02	0.225E-03	0.779E-03	0.106E-02	0.239E-02
4	0.670E-03	0.131E-02	0.276E-02	0.269E-01	0.161E-02	0.950E-02	-0.629E-02	-0.186E-01
5	-0.125E-03	0.993E-04	0.225E-03	0.161E-02	0.319E-03	0.774E-03	0.162E-02	0.457E-02
6	0.458E-03	0.405E-03	0.779E-03	0.950E-02	0.774E-03	0.776E-02	-0.675E-02	-0.163E-01
7	-0.341E-02	-0.767E-04	0.106E-02	-0.629E-02	0.162E-02	-0.675E-02	0.556E-01	0.125E+00
8	-0.866E-02	-0.331E-03	0.239E-02	-0.186E-01	0.457E-02	-0.163E-01	0.125E+00	0.336E+00

Table 7.5: Correlation coefficients $\left(\sigma_{ij}\right)\Big/\left(\sigma_{ii}\sigma_{jj}\right)^{1/2}$ from the combined F_2 and xF_3 fit. The parameter numbers are defined in Table 7.3.

#	GLOBAL	1	2	3	4	7	8	9	10
1	0.97237	1.000	0.005	-0.354	0.186	-0.318	0.236	-0.658	-0.680
2	0.99472	0.005	1.000	0.849	0.958	0.665	0.550	-0.039	-0.068
3	0.98531	-0.354	0.849	1.000	0.821	0.616	0.432	0.219	0.202
4	0.99737	0.186	0.958	0.821	1.000	0.549	0.658	-0.163	-0.196
7	0.95228	-0.318	0.665	0.616	0.549	1.000	0.492	0.385	0.442
8	0.94226	0.236	0.550	0.432	0.658	0.492	1.000	-0.325	-0.320
9	0.92182	-0.658	-0.039	0.219	-0.163	0.385	-0.325	1.000	0.918
10	0.95600	-0.680	-0.068	0.202	-0.196	0.442	-0.320	0.918	1.000

Table 7.6: QCD fit results as a function of the Q^2 cut on the data and the Q_0^2 of the evolution. "Prob" is the integrated upper tail of the χ^2 distribution for the given number of degrees of freedom (DOF). The $x < 0.7$ cut was applied to all the fits in this Table.

		xF_3-only fit			Combined F_2 and xF_3 fit			
Q_0^2	$Q_{\min}^2$	$\Lambda_{\overline{\text{MS}}}$	χ^2/DOF	Prob	$\Lambda_{\overline{\text{MS}}}$	η_G	χ^2/DOF	Prob
1	1	313 ± 39	124/106	11%	281 ± 12	2.83 ± 0.18	557/212	0%
1	5	390 ± 45	82/82	47%	272 ± 13	2.81 ± 0.33	366/164	0%
1	10	381 ± 47	59/59	49%	353 ± 28	3.17 ± 0.54	158/118	1%
1	15	392 ± 58	49/46	34%	392 ± 29	3.59 ± 0.64	107/ 92	13%
5	5	387 ± 42	81/82	50%	381 ± 24	4.44 ± 0.65	191/164	8%
5	10	422 ± 47	58/59	51%	381 ± 27	4.21 ± 1.55	138/118	10%
5	15	433 ± 53	50/46	31%	411 ± 37	4.00 ± 2.45	107/ 92	14%

Table 7.7: QCD fit results as a function of the x cut on the data. "Prob" is the integrated upper tail of the χ^2 distribution for the given number of degrees of freedom (DOF). $Q^2 = 5$ and $Q_0^2 = 5$ for all the fits in this Table.

	xF_3-only fit			Combined F_2 and xF_3 fit			
$x_{\max}$	$\Lambda_{\overline{\text{MS}}}$	χ^2/DOF	Prob	$\Lambda_{\overline{\text{MS}}}$	η_G	χ^2/DOF	Prob
.5	348 ± 49	62/70	74%	352 ± 27	4.99 ± 0.72	159/170	13%
.6	355 ± 43	72/77	65%	373 ± 23	4.62 ± 0.64	172/154	15%
.7	387 ± 42	81/82	50%	381 ± 24	4.44 ± 0.65	191/164	8%
.8	391 ± 40	86/86	48%	372 ± 20	4.61 ± 0.53	218/172	1%

The values of $\Lambda_{\overline{\rm MS}}$ from both fits are consistent with one another. This is an important check on the values of A_G and η_G, since the gluon distribution can only be determined indirectly by the co-evolution of the singlet and gluon distributions from Equation 7.13 and 7.14. The value of $\Lambda_{\overline{\rm MS}}$ and the shape of the gluon distribution are correlated: the correlation coefficient between $\Lambda_{\overline{\rm MS}}$ and η_G is 68%. If $\Lambda_{\overline{\rm MS}}$ from the non-singlet and combined fits had *not* agreed with each other, it might be concluded that the assumptions being made about the gluon shape and evolution were biasing the fit somehow. Since the values of $\Lambda_{\overline{\rm MS}}$ from the fits agree, it can be assumed that the values of A_G and η_G represent a valid measurement of the gluon distribution.

It is possible that the cuts made on the data have biased the QCD fit in some way. As a check, the QCD fits were repeated for different values of the x and Q^2 cut. Tables 7.6 and 7.7 show the results of this study. For the fits that evolve from $Q_0^2 = 1$, the poor χ^2 of the combined fit indicates that the predictions of perturbative QCD are not suitable for this kinematic region. For the fits that evolve from $Q_0^2 = 5$, the χ^2 of the combined fit does not lead to a "preferred" Q^2 cut, and so the fit with the greatest number of data points was chosen. For the fits for different x cuts, only the fit for $x < 0.8$ is poor, but the smearing corrections on the data at $x = 0.75$ are large, as noted in Section 6.1.3. The fit for $x < 0.7$ is chosen since the χ^2 is good and it includes the most data points.

Another possibility is that the choice of the functional form of the parameterization in Equation 7.1 may bias the fit to a particular value for $\Lambda_{\overline{\rm MS}}$. Table 7.8 shows the values of $\Lambda_{\overline{\rm MS}}$ determined from fits using different functional forms for q_{NS}. The results show that the value of $\Lambda_{\overline{\rm MS}}$ does not depend on the particular parameterization used in the fit. Table 7.9 shows the values for one set of alternate parameterizations.

Table 7.8: QCD fit results for xF_3-only fits for different functional forms of q_{NS}. "Prob" is the integrated upper tail of the χ^2 distribution for the given number of degrees of freedom (DOF). The $x < 0.7$ cut was applied, and $Q^2 = 5$ and $Q_0^2 = 5$ for all the fits in this Table. Functional form (1) was used for the results presented in this thesis; form (2) was used for the E616/E701 results reported in Ref. [Olt89]; form (3) was used in the preliminary QCD fits to the E744/E770 data [Qui92, Leu91]; form (4) was suggested [Zhi93] to look for two-nucleon correlations using QCD fits. The values of $\Lambda_{\overline{\rm MS}}$ obtained from using any of these functional forms are consistent with one another, and the χ^2 of the fits do not suggest that any of these forms should be preferred.

Number	xq_{NS}	$\Lambda_{\overline{\rm MS}}$	χ^2/DOF	Prob
1	$Ax^{\eta_1}(1-x)^{\eta_2}$	387 ± 42	81/82	50%
2	$Ax^{\eta_1}(1-x)^{\eta_2}(1+\gamma x)$	394 ± 41	80/81	50%
3	$Ax^{\eta_1}(1-x)^{\eta_2} + Bx^{\eta_3}$	387 ± 36	81/80	44%
4	$Ax^{\eta_1}(1-x)^{\eta_2} + Bx^{\eta_1}(1-x/2)^{\eta_3}$	390 ± 61	81/82	50%

Table 7.9: The values for one alternate parameterization of the parton distributions. "Prob" is the integrated upper tail of the χ^2 distribution for the given number of degrees of freedom (DOF). "FSR" is the value of the left-hand side of the integral in the Fermion Sum Rule in Equation 7.7. "MSR" is the value of the left-hand side of the integral of the Momentum Sum Rule in Equation 7.11. The values of $\Lambda_{\overline{\mathrm{MS}}}$ from both the xF_3-only and combined F_2 and xF_3 fit are consistent with one another. The alternate parameterizations used for this fit at $Q_0^2 = 5 GeV^2$ are

$$xq_{NS} = A_{NS} x^{\eta_1} (1-x)^{\eta_2} (1+\gamma x)$$
$$xq_S = xq_{NS} + A_S x^{\eta_R} (1-x)^{\eta_S} (1+\gamma_S x)$$
$$xG = A_G x^{\eta_F} (1-x)^{\eta_G} (1+\gamma_G x)$$

	xF_3-only fit	F_2 and xF_3 fit
$\Lambda_{\overline{\mathrm{MS}}}$ [MeV]	394 ± 41	368 ± 25
η_1	0.78 ± 0.03	0.78 ± 0.02
η_2	4.01 ± 0.12	3.99 ± 0.08
A_{NS}	8.00 ± 0.64	8.04 ± 0.52
γ	0.31 ± 0.33	0.25 ± 0.24
A_S		1.61 ± 0.13
η_R		0.02 ± 0.02
η_S		5.74 ± 0.36
γ_S		-1.79 ± 0.15
A_G		5.51 ± 3.61
η_F		0.33 ± 0.20
η_G		4.91 ± 1.29
γ_G		-1.44 ± 0.76
χ^2 / DOF	80 / 81	181 / 159
Prob	49%	11%
FSR	2.87	2.85
MSR		0.90

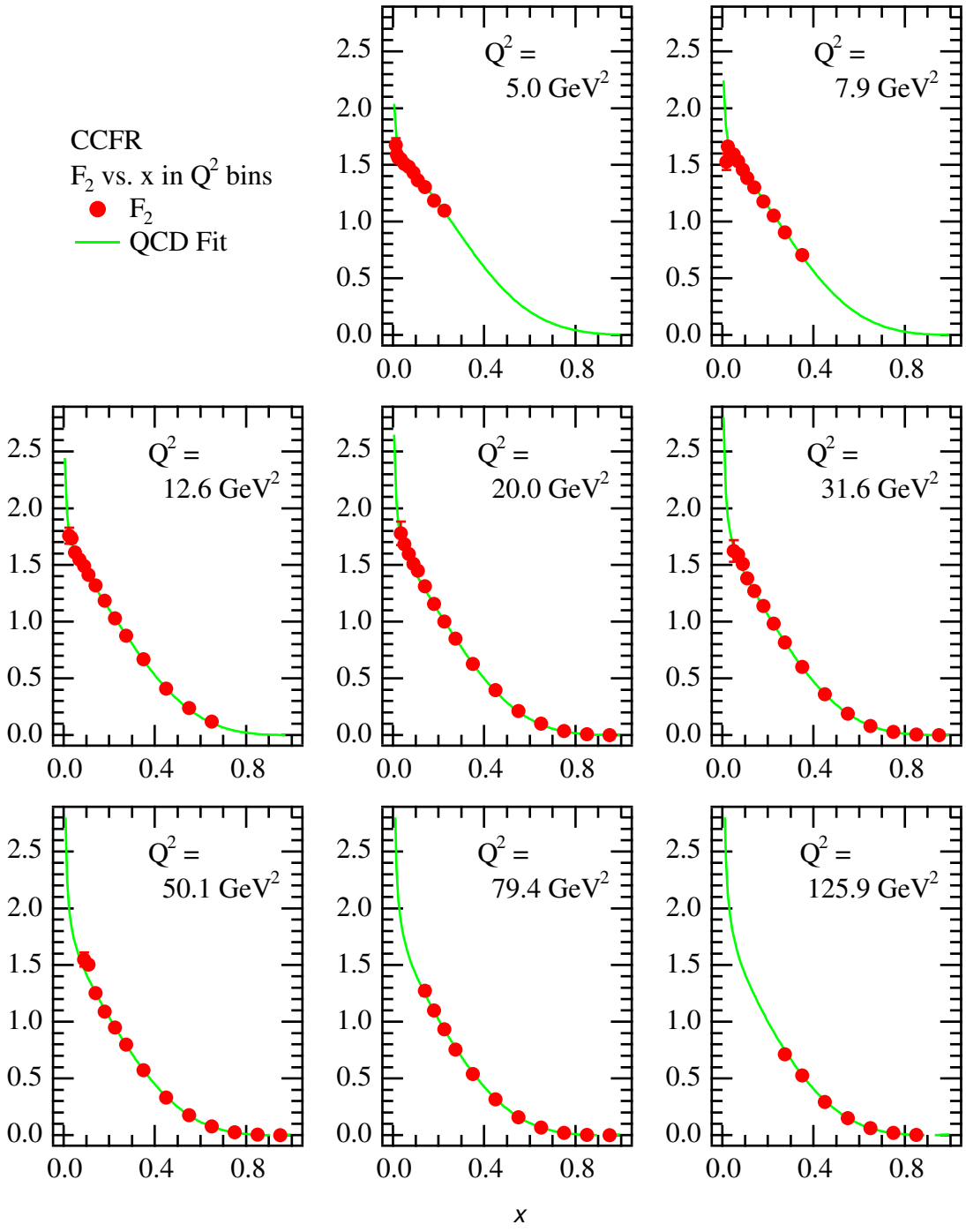

Figure 7.4: F_2 versus x in Q^2 bins. The line is the QCD fit to the data.

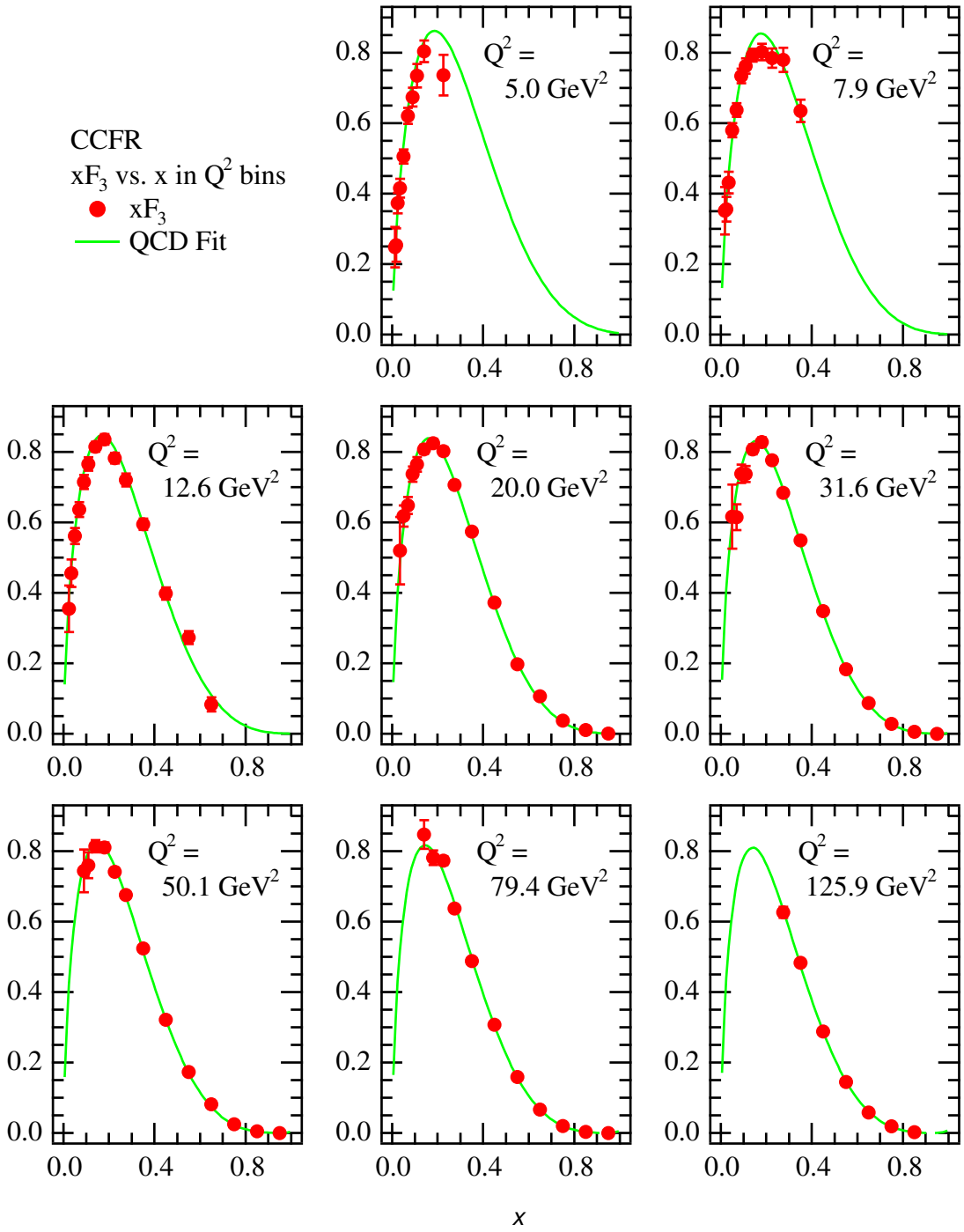

Figure 7.5: xF_3 versus x in Q^2 bins. The line is the QCD fit to the data.

7.2.2 Logarithmic Slopes

Plots of the logarithmic slopes provide a visual summary of the comparison between structure functions and QCD predictions, and verify that the data is consistent with the theory. These plots are also of historical significance, since the CCFR collaboration was the first to show agreement between the Q^2 evolution of both F_2 and xF_3 and the theory of QCD [Qui92].

The logarithmic slope of xF_3, $\left(d \ln xF_3\right) \Big/ \left(d \ln Q^2\right)$, is determined by fitting the xF_3 data separately within each *x*-bin to a power-law form:

$$xF_3\left(Q^2\right) = A \times \left(Q^2\right)^C \Rightarrow \frac{d \ln xF_3}{d \ln Q^2} = C \tag{7.35}$$

The relationship between $\Lambda_{\overline{\text{MS}}}$ and the logarithmic slopes is illustrated in Figure 7.6, which shows the slopes for xF_3 for different values of $\Lambda_{\overline{\text{MS}}}$. This family of curves shows that the value of $\Lambda_{\overline{\text{MS}}}$ is primarily determined by the high-*x* data. Since $F_2 \approx xF_3$ at $x >$ 0.5 (see Section 6.5), this implies that the value of $\Lambda_{\overline{\text{MS}}}$ from either the xF_3-only fit or the combined F_2 and xF_3 fit should be the same. Indeed, Table 7.1 shows that this is the case. Another consequence of the QCD theory is that the point in *x* at which the xF_3 slopes vanish should be almost independent of $\Lambda_{\overline{\text{MS}}}$ [Dev83]; this is seen in Figure 7.6. In leading-order QCD the "cross-over point" of the family of logarithmic slopes is exactly at $\left(d \ln xF_3\right) \Big/ \left(d \ln Q^2\right) = 0$, but this is shifted in NLO due to weak dependence of the splitting functions on α_S.

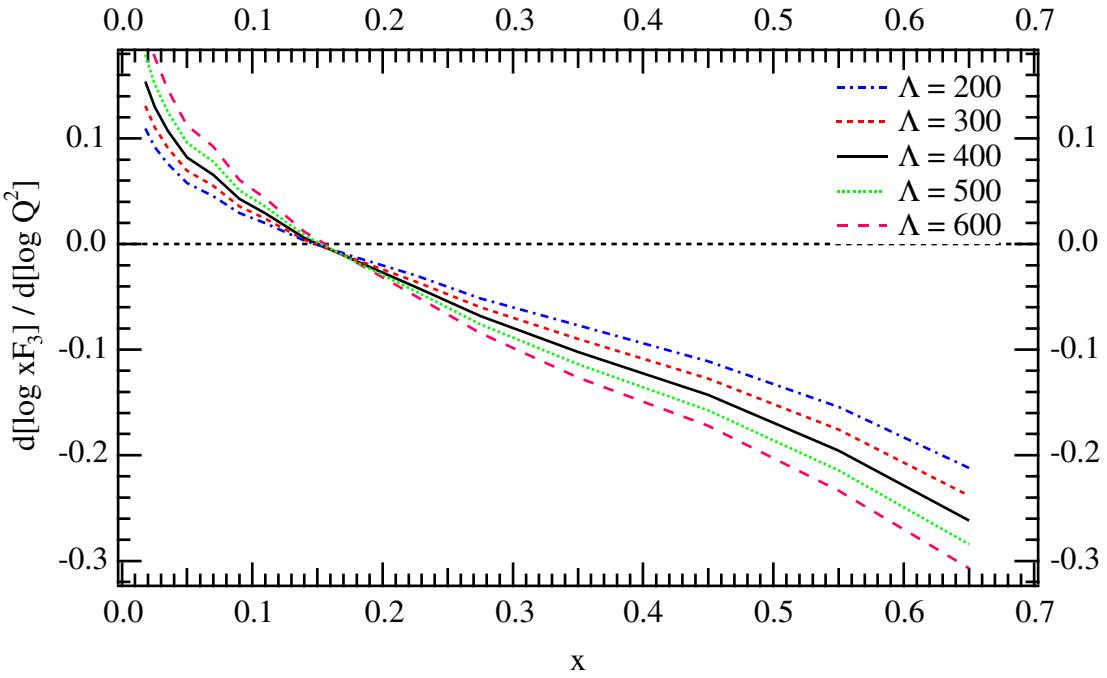

Figure 7.6: QCD prediction of logarithmic slopes of xF_3 for various values of Λ.

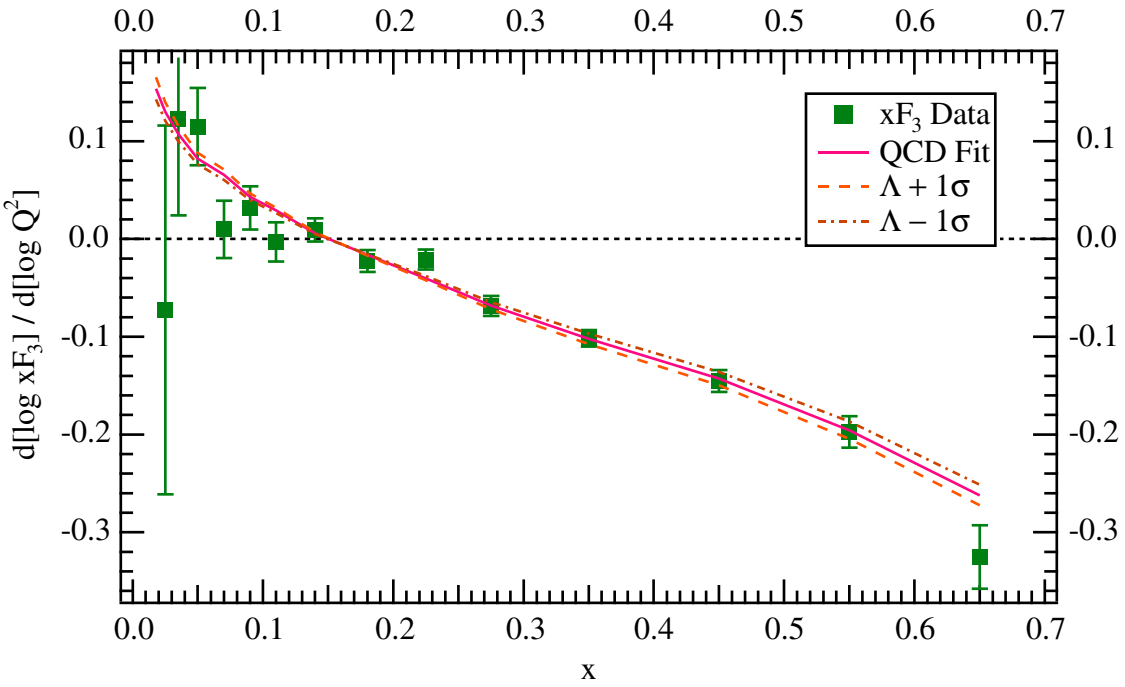

Figure 7.7: The logarithmic slopes of xF_3. The slopes from the QCD fit are plotted as a solid line. The $\pm 1\sigma$ variations in $\Lambda_{\overline{MS}} = 387 \pm 42\ MeV$ from the xF_3-only fit (dashed lines) are plotted to show the sensitivity of $\Lambda_{\overline{MS}}$ to the data.

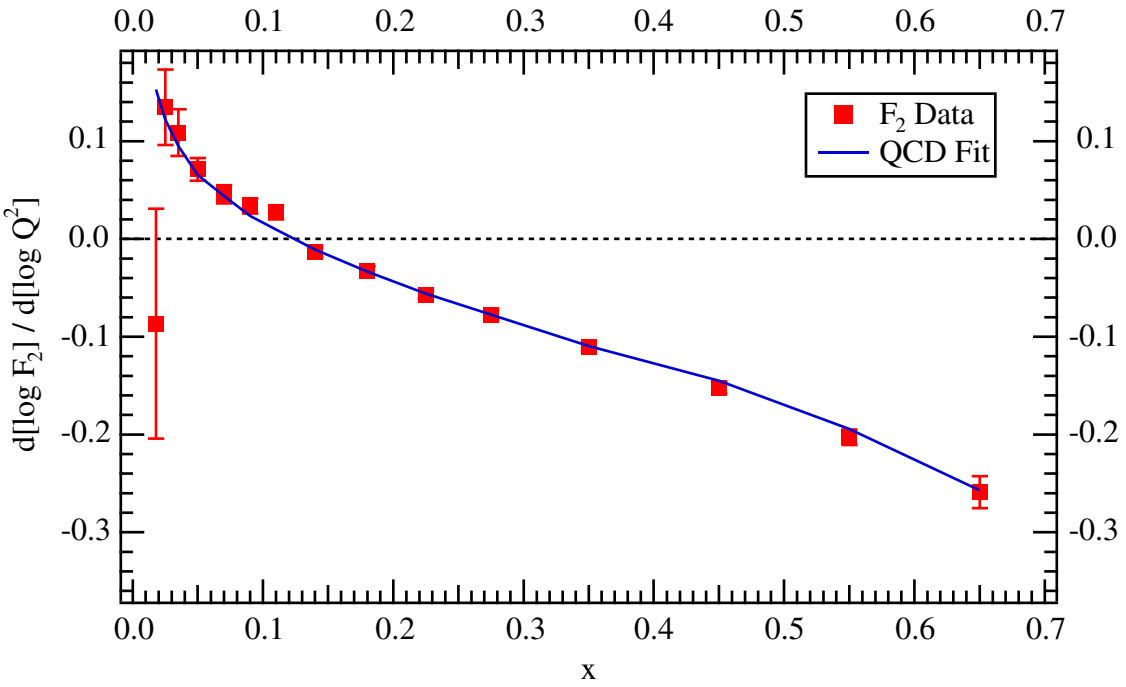

Figure 7.8: The logarithmic slopes of F_2. The slopes from the QCD fit are plotted as a solid line.

Figure 7.7 shows the comparison between the logarithmic slopes of xF_3 with the slopes from the xF_3-only QCD fit; the slopes for the $\pm 1\sigma$ variation in $\Lambda_{\overline{\text{MS}}}$ are also plotted. Figure 7.8 shows the corresponding plot for the slopes of F_2, with the QCD from the combined F_2 and xF_3 fit; the slopes for a $\pm 1\sigma$ $\Lambda_{\overline{\text{MS}}}$ variation are not included because on the scale of the plot a ±20 *MeV* shift would be barely visible.

7.2.3 Systematic Errors

This section discusses a basic approach to determining the systematic errors in the measurement of $\Lambda_{\overline{\text{MS}}}^{\text{NLO}}$. This approach is appropriate for *testing* QCD in the context of the systematic errors on the structure functions. Section 7.3 discusses another approach that *assumes* QCD and improves upon the measurement of $\Lambda_{\overline{\text{MS}}}^{\text{NLO}}$ in that context.

The experimental systematic errors are described in Section 6.4, and are listed in Table 7.10. The basic approach for determining the systematic error in $\Lambda_{\overline{\mathrm{MS}}}^{\mathrm{NLO}}$ due to the systematic error in a given quantity k is to fit F_k for the value of $\Lambda_{\overline{\mathrm{MS}}}^{\mathrm{NLO}}$, where F_k is obtained by extracting the structure functions with the systematic parameter changed by one standard error. Table 7.11 shows the variations in $\Lambda_{\overline{\mathrm{MS}}}^{\mathrm{NLO}}$ for each of the systematic errors for both the positive and negative systematic shifts, along with the χ^2 of the fit to F_k. Note that the variations of Λ_k are not necessarily symmetric about the central value Λ, nor is the shift in χ^2 necessarily the same for both the $\pm 1\delta$ variations; these asymmetries will be handled in the global systematic fit (see Section 7.3).

Table 7.12 shows the average systematic variation. The value of $\Lambda_{\overline{\mathrm{MS}}}^{\mathrm{NLO}}$ shown is the average of that obtained from a shift of $\pm 1\delta$ in the systematic quantity:

$$\frac{\left(\Lambda_k(1\delta)-\Lambda\right)}{\left|\left(\Lambda_k(1\delta)-\Lambda\right)\right|}\times\frac{\left|\left(\Lambda_k(1\delta)-\Lambda\right)\right|+\left|\left(\Lambda_k(-1\delta)-\Lambda\right)\right|}{2} \tag{7.36}$$

The total systematic error at the end of Table 7.12 is the sum of the individual systematic errors added in quadrature; the statistical and systematic errors in $\Lambda_{\overline{\mathrm{MS}}}^{\mathrm{NLO}}$ and η_G are summed in quadrature in the last line of the Table.

From Table 7.12, it can be seen that the largest source of systematic error in $\Lambda_{\overline{\mathrm{MS}}}^{\mathrm{NLO}}$ are the energy-calibration systematic errors, the muon-calibration error in particular, and the model parameterization error. The combined F_2 and xF_3 fit is, in general, less sensitive to systematic effects than the xF_3-only fit; the greatest reduction is in the systematic error due to $\sigma^{\bar{\nu}}/\sigma^{\nu}$.

Table 7.10: Systematic quantities and their $+1\delta$ variations as defined in Chapter 6. The percentage variation is given where appropriate.

Systematic Quantity	Central Value	$+1\delta$ Variation	Percentage Variation
C_{HAD}^{744}	Test Beam		1%
C_{HAD}^{770}	Test Beam		1%
ΔE_{HAD}	+150 *MeV*	100 *MeV*	
C_{μ}	Test Beam		1%
ΔE_{μ}	0	100 *MeV*	
$(B/A)_{744}^{\nu}$	-0.266	0.078	29%
$(B/A)_{744}^{\bar{\nu}}$	-1.682	0.041	2.4%
$(B/A)_{770}^{\nu}$	-0.324	0.069	21%
$(B/A)_{770}^{\bar{\nu}}$	--1.622	0.037	2.3%
σ^{ν}/E	0.677	0.014	2.1%
$\sigma^{\bar{\nu}}/\sigma^{\nu}$	0.499	0.007	1.4%
No Φ Adj		Adj. On/Off	
R_{World}	[Whi90b]		15%
m_c	1.31	0.24	18%
κ	0.373	0.046	12%
α	2.50	0.65	26%
B_c	0.105	0.007	7%
Model parameterization		On/Off	

Table 7.11: Variations in QCD fit results due to positive and negative systematic shifts. The values of $\Lambda = \Lambda^{\mathrm{NLO}}_{\overline{\mathrm{MS}}}$ and η_G for each systematic quantity varied by a positive and, if available, negative shift are listed. The units of $\Lambda^{\mathrm{NLO}}_{\overline{\mathrm{MS}}}$ are *MeV*. Note that not all systematic quantities have a negative variation defined. There were 82 degrees of freedom in the xF_3-only fit, and 164 DOF in the combined F_2 and xF_3 fit. The asymmetry in some variations and the χ^2 values is handled in the global systematic fit of Section 7.3.

	xF_3-only fit				Combined F_2 and xF_3 fit					
	+ shift		– shift		+ shift			– shift		
Systematic Quantity	Λ	χ^2	Λ	χ^2	Λ	η_G	χ^2	Λ	η_G	χ^2
C^{744}_{HAD}	–35	79	+30	88	–22	–0.03	189	+19	± 0.05	207
C^{770}_{HAD}	–32	86	+31	85	–16	–0.24	190	+29	–0.12	194
ΔE_{HAD}	–24	85	+21	85	–20	+0.15	189	+26	–0.32	198
C_μ	+45	84	–54	83	+38	–0.04	201	–21	–0.28	199
ΔE_μ	–08	85	+08	84	+04	–0.09	190	+05	–0.09	194
$(B/A)^{\nu}_{744}$	+14	82	–12	81	+07	–0.03	193	–07	+0.04	189
$(B/A)^{\bar{\nu}}_{744}$	–02	81	+03	82	+00	+0.04	191	–00	–0.04	191
$(B/A)^{\nu}_{770}$	+17	84	–14	84	+14	–0.18	193	–02	–0.07	189
$(B/A)^{\bar{\nu}}_{770}$	–01	84	+06	83	+06	–0.07	191	+05	–0.16	190
σ^{ν}/E	+00	81	–00	82	+00	+0.00	191	–00	–0.00	191
$\sigma^{\bar{\nu}}/\sigma^{\nu}$	–32	82	+29	84	+01	+0.21	190	–00	–0.22	198
No Φ Adj	–09	85			+00	–0.05	199			
R	–08	85	–10	86	+00	–0.04	199	+01	–0.05	200
m_c	+06	86			+10	–0.06	201			
κ	–11	86			–02	–0.07	200			
α	–08	85			+01	–0.19	200			
B_c	–12	86			–02	–0.04	199			
Model parameterization	+41	81			–06	+0.38	200			

Table 7.12: Statistical and average systematic errors in QCD fit results. The units of $\Lambda^{\rm NLO}_{\overline{\rm MS}}$ are *MeV*. The shifts in $\Lambda^{\rm NLO}_{\overline{\rm MS}}$ and η_G from Table 7.11 are averaged. A "±" variation means that if the systematic quantity is varied by $+1\delta$ as given in Table 7.10, the value of $\Lambda^{\rm NLO}_{\overline{\rm MS}}$ increased; a "$\overline{+}$" variation means that $\Lambda^{\rm NLO}_{\overline{\rm MS}}$ decreased.

	xF_3-only fit	Combined F_2 and xF_3 fit	
	$\Lambda^{\rm NLO}_{\overline{\rm MS}}$	$\Lambda^{\rm NLO}_{\overline{\rm MS}}$	η_G
Base ± Statistical Error	387 ± 42	381 ± 24	4.44 ± 0.65
Systematic Errors: C^{744}_{HAD}	$\overline{+}$ 32	$\overline{+}$ 21	± 0.04
C^{770}_{HAD}	$\overline{+}$ 32	$\overline{+}$ 23	$\overline{+}$ 0.18
ΔE_{HAD}	$\overline{+}$ 23	$\overline{+}$ 23	± 0.23
C_μ	± 49	± 30	$\overline{+}$ 0.16
ΔE_μ	$\overline{+}$ 08	± 04	± 0.09
$(B/A)^{\nu}_{744}$	± 13	± 07	$\overline{+}$ 0.04
$(B/A)^{\bar\nu}_{744}$	$\overline{+}$ 02	± 00	± 0.04
$(B/A)^{\nu}_{770}$	± 16	± 08	$\overline{+}$ 0.12
$(B/A)^{\bar\nu}_{770}$	$\overline{+}$ 03	± 06	$\overline{+}$ 0.12
σ^{ν}/E	± 00	± 00	± 0.00
$\sigma^{\bar\nu}/\sigma^{\nu}$	± 30	± 01	± 0.22
No Φ Adj	$\overline{+}$ 08	± 00	$\overline{+}$ 0.04
R	$\overline{+}$ 09	± 00	$\overline{+}$ 0.05
m_c	± 06	± 10	$\overline{+}$ 0.06
κ	$\overline{+}$ 11	$\overline{+}$ 02	$\overline{+}$ 0.07
α	$\overline{+}$ 08	± 01	$\overline{+}$ 0.19
B_c	$\overline{+}$ 12	$\overline{+}$ 02	$\overline{+}$ 0.04
Model parameterization	± 41	$\overline{+}$ 06	± 0.38
Total Systematic Error	± 93	± 51	± 0.63
Total Stat + Syst	± 102	± 56	± 0.91

Looking at the χ^2 of the different fits, it can be seen that none indicate a completely improbable fit. The poorest fit comes from the variation in m_c, which adds 5 units to the χ^2 of the xF_3-only fit, and 9 units to the χ^2 of the combined F_2 and xF_3 fit; however, the shift in $\Lambda_{\overline{\text{MS}}}^{\text{NLO}}$ due to the error in m_c is negligible. Overall, each individual systematically-varied fit is as consistent with QCD as the base fit, and so it is reasonable to conclude that the measurements of $\Lambda_{\overline{\text{MS}}}^{\text{NLO}}$ of $387 \pm 42 \pm 93$ *MeV* from the xF_3-only fit and $381 \pm 24 \pm 51$ *MeV* from the combined F_2 and xF_3 fit are both consistent with QCD. Since there is no reason not to select the result with the smaller statistical and systematic errors, the result of this basic approach to QCD fits is a value for $\Lambda_{\overline{\text{MS}}}^{\text{NLO}}$ of 381 ± 56 *MeV* (stat. + syst.) with a gluon distribution shape parameter η_G given by 4.44 ± 0.91 (stat. + syst.).

Given the systematic differences in $\sigma^{\bar{\nu}} / \sigma^{\nu}$ between E744 and E770 described in Section 5.3.1, it is worth examining the values of $\Lambda_{\overline{\text{MS}}}^{\text{NLO}}$ determined from each experiment separately. The results of separate QCD fits are shown in Table 7.13. The results of the individual experiments are consistent with each other and with the fits to both experiments combined.

Table 7.13: Results from separate QCD fits to experiments E744 and E770.

	xF_3-only fit		Combined F_2 and xF_3 fit		
	$\Lambda_{\overline{\text{MS}}}^{\text{NLO}}$	χ^2/DOF	$\Lambda_{\overline{\text{MS}}}^{\text{NLO}}$	η_G	χ^2/DOF
E744	398 ± 64	74/81	378 ± 25	3.80 ± 0.69	140/162
E770	391 ± 53	98/82	383 ± 30	5.15 ± 0.96	201/164
Both E744 + E770	387 ± 42	81/82	387 ± 24	4.44 ± 0.65	191/164

7.3 Global Systematic Fits

There are three approaches one can take when incorporating systematic errors in a fit of the structure functions to a theoretical model.

- The systematic errors can be together added in quadrature to the statistical error for each data point. This is the approach taken by most of the global fits that include the CCFR data [Lai96]. This approach ignores the point-to-point correlations between the systematic errors; for example, it assumes that one can vary $\sigma^{\bar{\nu}}/\sigma^{\nu}$ for one (x,Q^2) bin independently of $\sigma^{\bar{\nu}}/\sigma^{\nu}$ in an adjacent bin. This technique will overestimate the systematic errors, and it is not used in this thesis since the technique is patently wrong.

- Each structure function that has been varied by a systematic quantity k can be fit separately. The results of each of the fits can then be added in quadrature. This is the approach used in the previous section. This approach takes into account the point-to-point correlations of a systematic error, and can be used to test the agreement of the data with the QCD model. However, it ignores the possibility of correlations between the systematic errors. Also, Table 7.12 suggests that the effects of the systematic errors are being overestimated. For example, a 1δ shift in C_{HAD}^{770} adds 4 units to the χ^2 of the xF_3-only fit. This technique is not using the information in the structure-function data that could limit the C_{HAD}^{770} systematic uncertainty.

- The third approach, defined fully below, incorporates the systematic variations in the structure functions as part of the fit. As shown below, this approach tests to see if there are any correlations between the systematic errors, uses the data to test whether the limits assigned to the systematic variations are conservative, and reduces the size

of overall error due to systematic effects in comparison to the previous approach. However, this approach cannot test the theory of QCD. The theory is assumed to be true, and the fit is extracting the parameters of the theory with the best precision. This is appropriate because the quantity being measured by the fit, $\Lambda_{\overline{\mathrm{MS}}}^{NLO,(4)}$, *only* has meaning in the context of the theory of QCD.

The global systematic error fit incorporates the systematic errors described in Section 6.4 in the QCD fit. Each δ_k associated with a systematically-varied structure function becomes a MINUIT parameter. The χ^2 of Equations 7.32-7.33 is replaced by

$$\vec{\mathbf{F}}^{diff} = \vec{\mathbf{F}}^{data} - \vec{\mathbf{F}}^{theory} + \sum_k \delta_k \left(\vec{\mathbf{F}}^{k} - \vec{\mathbf{F}}^{data} \right) \tag{7.37}$$

$$\chi^2 = \sum_{(x,Q^2)\text{bins}} \left(\vec{\mathbf{F}}^{diff} \right)^{\mathrm{T}} \hat{\mathbf{V}}^{-1} \left(\vec{\mathbf{F}}^{diff} \right) + \sum_k \delta_k^2 \tag{7.38}$$

With this definition, the value of δ_k determined by MINUIT is the fraction of the shift between the base structure function $\vec{\mathbf{F}}$ and the structure function varied by one unit of the systematic quantity, $\vec{\mathbf{F}}^{k}$. If, for example, the MINUIT fit reported that $\delta\left(\sigma^{\bar{\nu}} / \sigma^{\nu}\right) = 1.0$, then it would imply that the best fit to the data is found when $\sigma^{\bar{\nu}} / \sigma^{\nu}$ is varied by +14%, the definition of one unit of systematic variation defined in Chapter 6 and shown in Table 7.10. The inclusion of the $\sum \delta_k^2$ term in Equation 7.38 means that MINUIT must pay a χ^2 "penalty" for varying the data by any of the systematic quantities, and that δ_k typically varies between –1 and +1.

The one systematic error not included in the global systematic fit is that in the overall neutrino-iron cross-section, σ^{ν} / E. The reason is that, when used as a MINUIT parameter, it is highly correlated with A_{NS}, A_S, and A_G, the normalizations for the parton distributions. Since only one overall normalization parameter is necessary for the

fit, the parton distribution normalizations were picked as parameters so the results could be compared directly with the results in Table 7.1.

The results of the global systematic fit are shown in Table 7.14. The error matrix from the xF_3-only fit is shown in Table 7.15, and the correlation coefficients are shown in Table 7.16. The error matrix from the combined F_2 and xF_3 fit is shown in Table 7.17, and the correlation coefficients are shown in Table 7.18.

The error in δ_k reported by MINUIT reflects what improvement, if any, the given systematic error on that parameter can be reduced in context of the theory of QCD. If the error in δ_k is close to 1, then the global fit cannot improve upon the error defined in Section 6.4. For example, the error in $\delta\left(B_c\right)$ is 0.92 for the xF_3-only fit; this implies that the charged-current data in combination with the QCD model for the inclusive cross-section cannot improve upon the error of 7% determined for the charm branching ratio B_c from the dimuon analysis [Rab93].

In contrast, the error in $\delta\left(C_\mu\right)$ is 0.22 for the xF_3-only fit. The systematic error for C_μ from Table 7.10 is 1%. Therefore, the structure-function data in combination with QCD is able to reduce that systematic error to $0.22 \times 1\% = 0.22\%$. The reason for this reduction is that the value of $Q^2 \approx E_\nu E_\mu \theta_\mu^2$ is sensitive to the muon calibration. This changes the value of $d \ln xF_3 \,/\, d \ln Q^2$, which in turn affects the value of $\alpha_S(Q^2)$ and $\Lambda_{\overline{\mathrm{MS}}}$ according to Equation 7.12. Also, as shown in Figure 5.10, changing the muon energy calibration also changes the shape of the flux. Q^2 is also sensitive to the E_{HAD} calibration, since $E_\nu = E_{HAD} + E_\mu$, and so the systematic error in the hadron energy calibration is also reduced by the global fit. Note that though the error in C_μ is reduced its central value is not shifted. However, the error in C_{HAD}^{744} is reduced and its central value is shifted outside that reduced error.

Table 7.14: Results of the global systematic QCD fit. "Prob" is the integrated upper tail of the χ^2 distribution for the given number of degrees of freedom (DOF). "FSR" is the value of the left-hand side of the integral in the Fermion Sum Rule in Equation 7.7. "MSR" is the value of the left-hand side of the integral in Equation 7.11.

Number		xF_3-only fit	F_2 and xF_3 fit
1	$\Lambda_{\overline{\text{MS}}}$ [MeV]	381 ± 53	337 ± 28
2	η_1	0.794 ± 0.011	0.804 ± 0.009
3	η_2	3.88 ± 0.03	3.94 ± 0.03
4	A_{NS}	8.40 ± 0.21	8.60 ± 0.18
7	A_S		1.47 ± 0.04
8	η_S		7.67 ± 0.13
9	A_G		2.22 ± 0.34
10	η_G		4.66 ± 0.68
11	$\delta\left(C_{HAD}^{744}\right)$	1.01 ± 0.53	0.95 ± 0.42
12	$\delta\left(C_{HAD}^{770}\right)$	-0.10 ± 0.45	0.28 ± 0.27
20	$\delta\left(\Delta E_{HAD}\right)$	-0.03 ± 0.71	0.79 ± 0.44
21	$\delta\left(C_\mu\right)$	0.22 ± 0.25	0.21 ± 0.18
22	$\delta\left(\Delta E_\mu\right)$	0.11 ± 0.60	-0.15 ± 0.36
23	$\delta\left((B/A)_{744}^{\nu}\right)$	0.12 ± 0.94	-0.31 ± 0.91
24	$\delta\left((B/A)_{744}^{\bar{\nu}}\right)$	0.02 ± 0.99	-0.01 ± 0.98
25	$\delta\left((B/A)_{770}^{\nu}\right)$	-0.03 ± 0.71	0.18 ± 0.56
26	$\delta\left((B/A)_{770}^{\bar{\nu}}\right)$	0.13 ± 0.82	0.46 ± 0.70
30	$\delta\left(\sigma^{\bar{\nu}}/\sigma^{\nu}\right)$	-0.13 ± 0.64	0.04 ± 0.50
31	$\delta(\text{No}\Phi\text{Adj})$	0.08 ± 0.92	0.18 ± 0.73
32	$\delta(R)$	0.03 ± 0.91	-0.22 ± 0.42
33	$\delta\left(m_c\right)$	-0.34 ± 0.87	-1.22 ± 0.77
34	$\delta(\kappa)$	0.14 ± 0.92	0.37 ± 0.90
35	$\delta(\alpha)$	0.07 ± 0.92	-0.08 ± 0.88
36	$\delta\left(B_c\right)$	0.20 ± 0.92	0.09 ± 0.89
37	δ(model)	0.50 ± 0.20	0.44 ± 0.12
	χ^2 / DOF	69 / 82	157 / 164
	Prob	85%	62%
	FSR	2.84	2.80
	MSR		0.96

Table 7.15: The error matrix σ_{ij} from the xF_3-only global systematic fit. The elements above the diagonal are not printed. The parameter numbers are defined in Table 7.14. For space reasons, the column values "wrap around" to succeeding rows starting with parameter 25.

	1	2	3	4	11	12	20	21	22	23	24
1	0.203E-02										
2	-0.418E-04	0.131E-03									
3	-0.801E-03	0.238E-03	0.118E-02								
4	0.205E-02	0.202E-02	0.415E-02	0.424E-01							
11	-0.423E-02	-0.582E-03	0.723E-03	-0.139E-01	0.291E+00						
12	-0.140E-02	0.690E-03	0.300E-02	0.161E-01	-0.353E-01	0.198E+00					
20	-0.224E-02	0.293E-03	0.964E-03	0.874E-02	-0.854E-02	-0.364E-01	0.498E+00				
21	-0.107E-02	0.333E-03	-0.273E-02	-0.709E-02	0.365E-01	0.841E-02	0.121E-01	0.610E-01			
22	-0.295E-02	0.125E-03	0.138E-02	0.876E-02	-0.484E-01	-0.147E-01	-0.105E+00	-0.404E-01	0.365E+00		
23	0.418E-02	0.179E-02	0.193E-02	0.169E-01	0.606E-02	0.194E-01	-0.143E-02	-0.132E-01	0.217E-01	0.889E+00	
24	0.547E-03	-0.124E-02	-0.173E-02	-0.139E-01	-0.175E-02	0.346E-02	-0.228E-02	-0.553E-03	-0.563E-02	0.404E-01	0.977E+00
25	0.484E-02	-0.312E-03	-0.923E-03	-0.396E-02	0.507E-01	-0.317E-01	-0.111E+00	-0.222E-01	-0.349E-01	-0.653E-01	0.108E-01
	0.498E+00										
26	-0.935E-03	0.159E-03	0.116E-02	0.416E-02	0.566E-01	-0.406E-02	-0.139E+00	-0.249E-02	-0.455E-01	-0.401E-01	0.135E-01
	-0.237E+00	0.671E+00									
30	-0.568E-02	0.344E-02	0.370E-02	0.108E-01	-0.233E-01	-0.177E-01	-0.907E-02	0.346E-01	-0.605E-01	0.142E+00	-0.753E-01
	0.376E-01	-0.639E-02	0.405E+00								
31	-0.135E-02	-0.308E-04	0.544E-03	-0.708E-02	-0.919E-02	-0.157E-01	-0.163E-01	0.334E-02	-0.107E-01	-0.364E-02	0.586E-02
	-0.125E-01	-0.427E-01	0.383E-01	0.844E+00							
32	-0.113E-02	0.763E-04	0.708E-03	-0.514E-02	-0.144E-01	-0.166E-01	-0.898E-02	0.204E-02	-0.176E-01	-0.280E-02	0.335E-02
	-0.235E-01	-0.279E-01	0.228E-01	-0.153E+00	0.833E+00						
33	0.102E-01	0.780E-03	-0.537E-02	0.281E-01	0.785E-02	-0.161E-02	-0.107E-01	0.133E-02	-0.185E-01	0.624E-01	-0.294E-01
	0.993E-02	-0.239E-01	-0.569E-01	-0.140E+00	-0.140E+00	0.761E+00					
34	-0.243E-02	-0.107E-02	-0.358E-03	-0.205E-01	-0.838E-02	-0.152E-01	-0.200E-01	0.466E-02	-0.150E-01	0.137E-01	-0.459E-02
	-0.738E-02	-0.411E-01	-0.113E-01	-0.150E+00	-0.148E+00	-0.152E+00	0.848E+00				
35	-0.122E-02	-0.525E-04	0.389E-03	-0.900E-02	-0.825E-02	-0.160E-01	-0.145E-01	0.210E-02	-0.872E-02	-0.643E-02	0.709E-02
	-0.140E-01	-0.431E-01	0.493E-01	-0.157E+00	-0.153E+00	-0.139E+00	-0.150E+00	0.842E+00			
36	-0.241E-02	-0.514E-03	0.135E-03	-0.114E-01	-0.958E-02	-0.173E-01	-0.198E-01	0.636E-02	-0.166E-01	0.198E-01	-0.502E-02
	-0.385E-02	-0.394E-01	-0.170E-01	-0.152E+00	-0.150E+00	-0.152E+00	-0.152E+00	-0.151E+00	0.846E+00		
37	0.194E-02	-0.450E-03	-0.642E-03	-0.814E-02	0.228E-02	-0.119E-01	-0.156E-01	-0.152E-02	-0.194E-01	0.143E-02	-0.228E-02
	0.711E-02	-0.749E-02	0.999E-03	0.504E-02	0.523E-02	0.257E-02	0.287E-02	0.489E-02	0.393E-02	0.400E-01	

Table 7.16: Correlation coefficients $\left(\sigma_{ij}\right)\Big/\left(\sigma_{ii}\sigma_{jj}\right)^{1/2}$ for the xF_3-only global systematic fit. The parameter numbers are defined in Table 7.14. For space reasons, the column values "wrap around" to succeeding rows starting with parameter 33.

NO.	GLOBAL	1	2	3	4	11	12	20	21	22	23	24	25	26	30	31	32
1	0.98300	1.000	-0.081	-0.518	0.220	-0.174	-0.070	-0.071	-0.096	-0.108	0.098	0.012	0.152	-0.025	-0.198	-0.033	-0.028
2	0.98915	-0.081	1.000	0.608	0.857	-0.094	0.136	0.036	0.118	0.018	0.166	-0.109	-0.039	0.017	0.474	-0.003	0.007
3	0.98375	-0.518	0.608	1.000	0.588	0.039	0.197	0.040	-0.322	0.067	0.060	-0.051	-0.038	0.041	0.170	0.017	0.023
4	0.99445	0.220	0.857	0.588	1.000	-0.125	0.176	0.060	-0.139	0.070	0.087	-0.068	-0.027	0.025	0.082	-0.037	-0.027
11	0.63028	-0.174	-0.094	0.039	-0.125	1.000	-0.147	-0.022	0.273	-0.148	0.012	-0.003	0.133	0.128	-0.068	-0.019	-0.029
12	0.79387	-0.070	0.136	0.197	0.176	-0.147	1.000	-0.116	0.076	-0.055	0.046	0.008	-0.101	-0.011	-0.063	-0.038	-0.041
20	0.89843	-0.071	0.036	0.040	0.060	-0.022	-0.116	1.000	0.070	-0.246	-0.002	-0.003	-0.224	-0.240	-0.020	-0.025	-0.014
21	0.85322	-0.096	0.118	-0.322	-0.139	0.273	0.076	0.070	1.000	-0.271	-0.057	-0.002	-0.127	-0.012	0.220	0.015	0.009
22	0.86761	-0.108	0.018	0.067	0.070	-0.148	-0.055	-0.246	-0.271	1.000	0.038	-0.009	-0.082	-0.092	-0.158	-0.019	-0.032
23	0.64725	0.098	0.166	0.060	0.087	0.012	0.046	-0.002	-0.057	0.038	1.000	0.043	-0.098	-0.052	0.236	-0.004	-0.003
24	0.20852	0.012	-0.109	-0.051	-0.068	-0.003	0.008	-0.003	-0.002	-0.009	0.043	1.000	0.016	0.017	-0.120	0.006	0.004
25	0.89545	0.152	-0.039	-0.038	-0.027	0.133	-0.101	-0.224	-0.127	-0.082	-0.098	0.016	1.000	-0.411	0.084	-0.019	-0.036
26	0.91986	-0.025	0.017	0.041	0.025	0.128	-0.011	-0.240	-0.012	-0.092	-0.052	0.017	-0.411	1.000	-0.012	-0.057	-0.037
30	0.89713	-0.198	0.474	0.170	0.082	-0.068	-0.063	-0.020	0.220	-0.158	0.236	-0.120	0.084	-0.012	1.000	0.066	0.039
31	0.94920	-0.033	-0.003	0.017	-0.037	-0.019	-0.038	-0.025	0.015	-0.019	-0.004	0.006	-0.019	-0.057	0.066	1.000	-0.183
32	0.94873	-0.028	0.007	0.023	-0.027	-0.029	-0.041	-0.014	0.009	-0.032	-0.003	0.004	-0.036	-0.037	0.039	-0.183	1.000
33	0.94784	0.259	0.078	-0.179	0.157	0.017	-0.004	-0.017	0.006	-0.035	0.076	-0.034	0.016	-0.033	-0.103	-0.174	-0.176
		1.000	-0.189	-0.174	-0.190	0.015											
34	0.94963	-0.059	-0.102	-0.011	-0.108	-0.017	-0.037	-0.031	0.020	-0.027	0.016	-0.005	-0.011	-0.054	-0.019	-0.177	-0.176
		-0.189	1.000	-0.177	-0.179	0.016											
35	0.94901	-0.029	-0.005	0.012	-0.048	-0.017	-0.039	-0.022	0.009	-0.016	-0.007	0.008	-0.022	-0.057	0.084	-0.186	-0.183
		-0.174	-0.177	1.000	-0.180	0.027											
36	0.95019	-0.058	-0.049	0.004	-0.060	-0.019	-0.042	-0.030	0.028	-0.030	0.023	-0.006	-0.006	-0.052	-0.029	-0.180	-0.178
		-0.190	-0.179	-0.180	1.000	0.021											
37	0.79060	0.214	-0.197	-0.094	-0.198	0.021	-0.134	-0.111	-0.031	-0.161	0.008	-0.012	0.050	-0.046	0.008	0.027	0.029
		0.015	0.016	0.027	0.021	1.000											

Table 7.17: The error matrix σ_{ij} from the combined F_2 and xF_3 global systematic fit. The elements above the diagonal are not printed. The parameter numbers are defined in Table 7.14. For space reasons, the column values "wrap around" to succeeding rows starting with parameter 21.

	1	2	3	4	7	8	9	10	11	12	20
1	0.545E-03										
2	0.118E-04	0.878E-04									
3	-0.384E-03	0.156E-03	0.796E-03								
4	0.429E-04	0.147E-02	0.346E-02	0.289E-01							
7	0.347E-03	0.179E-03	0.224E-03	0.389E-02	0.103E-02						
8	-0.286E-03	0.158E-03	0.110E-02	0.854E-02	0.220E-02	0.154E-01					
9	-0.323E-02	-0.276E-05	0.339E-02	0.399E-02	-0.217E-02	0.291E-02	0.524E-01				
10	-0.258E-02	0.748E-04	0.308E-02	0.358E-02	-0.288E-02	-0.829E-03	0.569E-01	0.156E+00			
11	-0.166E-02	-0.126E-04	0.153E-02	0.255E-02	-0.300E-03	0.308E-02	0.120E-01	-0.446E-01	0.175E+00		
12	-0.691E-03	0.110E-03	0.122E-02	0.391E-02	-0.422E-03	0.384E-04	0.772E-02	-0.364E-02	-0.263E-02	0.710E-01	
20	-0.195E-02	0.158E-03	0.232E-02	0.541E-02	0.816E-04	-0.248E-02	-0.127E-03	0.501E-02	-0.416E-02	-0.216E-01	0.190E+00
21	0.946E-03	-0.955E-04	-0.261E-02	-0.620E-02	-0.122E-02	-0.344E-02	-0.117E-01	-0.110E-01	0.167E-01	0.270E-02	-0.512E-02
	0.312E-01										
22	-0.607E-03	-0.144E-03	-0.720E-04	-0.225E-03	0.601E-03	0.647E-02	0.571E-02	0.338E-02	-0.203E-02	-0.118E-01	-0.263E-01
	-0.137E-01	0.133E+00									
23	0.389E-02	0.102E-02	0.684E-03	0.568E-02	0.181E-02	-0.185E-01	-0.398E-01	0.747E-02	0.312E-01	0.113E-01	-0.174E-02
	-0.163E-01	0.194E-01	0.829E+00								
24	-0.642E-03	-0.100E-02	-0.616E-03	-0.128E-01	-0.198E-02	0.589E-02	0.223E-02	0.483E-01	0.570E-02	0.257E-02	-0.254E-02
	0.194E-02	-0.295E-02	0.469E-01	0.962E+00							
25	0.135E-02	0.695E-04	-0.565E-03	-0.936E-03	0.213E-02	-0.222E-02	-0.488E-02	-0.894E-02	0.200E-01	-0.113E-01	-0.174E-01
	-0.838E-02	-0.846E-02	-0.308E-01	0.589E-02	0.311E+00						
26	-0.277E-03	0.253E-04	0.927E-03	0.452E-02	-0.855E-03	0.178E-02	0.786E-02	-0.986E-02	0.416E-01	0.151E-01	-0.888E-01
	0.161E-03	-0.417E-01	-0.406E-01	0.525E-02	-0.225E+00	0.497E+00					
30	0.357E-02	0.178E-02	-0.151E-02	0.926E-02	0.834E-03	-0.394E-01	-0.287E-01	-0.158E-01	-0.273E-01	-0.108E-01	-0.250E-02
	0.484E-02	-0.219E-01	0.108E+00	-0.558E-01	0.282E-01	-0.251E-01	0.249E+00				
31	-0.326E-02	0.195E-05	0.480E-03	-0.102E-01	-0.244E-02	-0.152E-01	0.233E-01	0.107E+00	-0.321E-02	0.579E-02	0.471E-02
	0.591E-02	-0.101E-01	0.716E-02	-0.656E-02	-0.269E-01	-0.255E-01	0.434E-01	0.533E+00			
32	0.101E-02	0.360E-04	-0.380E-03	0.179E-02	0.405E-02	0.142E-01	0.629E-02	-0.145E-01	0.601E-02	-0.346E-01	-0.124E-01
	-0.622E-02	0.121E-01	-0.526E-02	0.471E-02	0.336E-01	-0.152E-01	-0.483E-02	-0.367E-01	0.174E+00		
33	0.114E-01	0.106E-02	-0.382E-02	0.370E-01	0.163E-01	0.297E-01	-0.104E+00	-0.116E+00	-0.216E-01	0.723E-03	-0.136E-01
	0.364E-02	-0.236E-02	0.435E-01	-0.281E-01	0.223E-02	-0.212E-01	-0.464E-01	-0.349E-01	-0.429E-01	0.586E+00	
34	-0.528E-02	-0.101E-02	0.760E-03	-0.256E-01	-0.781E-02	-0.130E-01	0.522E-01	0.878E-01	-0.206E-02	-0.130E-02	-0.345E-02
	-0.254E-02	-0.614E-03	-0.248E-01	0.123E-01	-0.103E-01	-0.257E-01	0.103E-01	0.157E+00	0.289E-02	-0.230E+00	0.175E+00
35	0.155E-03	0.677E-04	-0.261E-02	-0.120E-01	-0.646E-02	-0.172E-01	0.308E-02	-0.675E-02	-0.243E-01	-0.575E-02	-0.230E-01
	0.274E-01	-0.144E-01	0.167E-01	-0.148E-02	-0.162E-01	-0.260E-01	0.566E-01	-0.219E+00	-0.261E-01	-0.166E+00	0.192E-02
	0.277E+00										
36	-0.243E-02	-0.370E-03	0.289E-02	-0.464E-03	-0.418E-02	0.218E-02	0.106E-01	-0.450E-01	-0.715E-02	0.476E-02	0.149E-01
	-0.173E-01	-0.406E-02	0.142E-01	0.794E-02	-0.781E-02	-0.299E-01	-0.378E-01	-0.354E+00	-0.402E-01	-0.876E-01	-0.625E-01
	0.201E+00	0.369E+00									
37	-0.223E-04	0.393E-04	0.197E-03	-0.641E-03	-0.666E-03	-0.245E-02	-0.101E-02	0.474E-02	-0.310E-02	-0.133E-02	0.493E-02
	0.684E-03	-0.244E-02	0.202E-02	0.617E-03	-0.101E-01	0.145E-03	0.200E-02	0.229E-02	-0.579E-02	0.134E-02	-0.170E-02
	0.136E-02	0.346E-02	0.148E-01								

Table 7.18: Correlation coefficients $\left(\sigma_{ij}\right)\Big/\left(\sigma_{ii}\sigma_{jj}\right)^{1/2}$ for the combined F_2 and xF_3 global systematic fit. The parameter numbers are defined in Table 7.14. For space reasons, the column values "wrap around" to succeeding rows starting with parameter 26.

NO.	GLOBAL	1	2	3	4	7	8	9	10	11	12	20	21	22	23	24	25
1	0.97903	1.000	0.054	-0.584	0.011	0.464	-0.099	-0.604	-0.280	-0.170	-0.111	-0.192	0.229	-0.071	0.183	-0.028	0.104
2	0.99595	0.054	1.000	0.591	0.923	0.597	0.136	-0.001	0.020	-0.003	0.044	0.039	-0.058	-0.042	0.120	-0.109	0.013
3	0.99238	-0.584	0.591	1.000	0.721	0.248	0.313	0.525	0.276	0.130	0.162	0.189	-0.523	-0.007	0.027	-0.022	-0.036
4	0.99776	0.011	0.923	0.721	1.000	0.714	0.405	0.102	0.053	0.036	0.086	0.073	-0.207	-0.004	0.037	-0.077	-0.010
7	0.98834	0.464	0.597	0.248	0.714	1.000	0.554	-0.296	-0.227	-0.022	-0.049	0.006	-0.215	0.051	0.062	-0.063	0.119
8	0.97251	-0.099	0.136	0.313	0.405	0.554	1.000	0.103	-0.017	0.059	0.001	-0.046	-0.157	0.143	-0.163	0.048	-0.032
9	0.91376	-0.604	-0.001	0.525	0.102	-0.296	0.103	1.000	0.628	0.125	0.127	-0.001	-0.289	0.068	-0.191	0.010	-0.038
10	0.91506	-0.280	0.020	0.276	0.053	-0.227	-0.017	0.628	1.000	-0.270	-0.035	0.029	-0.158	0.023	0.021	0.125	-0.041
11	0.86603	-0.170	-0.003	0.130	0.036	-0.022	0.059	0.125	-0.270	1.000	-0.024	-0.023	0.226	-0.013	0.082	0.014	0.086
12	0.83339	-0.111	0.044	0.162	0.086	-0.049	0.001	0.127	-0.035	-0.024	1.000	-0.186	0.057	-0.121	0.047	0.010	-0.076
20	0.90640	-0.192	0.039	0.189	0.073	0.006	-0.046	-0.001	0.029	-0.023	-0.186	1.000	-0.067	-0.166	-0.004	-0.006	-0.072
21	0.93693	0.229	-0.058	-0.523	-0.207	-0.215	-0.157	-0.289	-0.158	0.226	0.057	-0.067	1.000	-0.212	-0.101	0.011	-0.085
22	0.85208	-0.071	-0.042	-0.007	-0.004	0.051	0.143	0.068	0.023	-0.013	-0.121	-0.166	-0.212	1.000	0.059	-0.008	-0.042
23	0.82669	0.183	0.120	0.027	0.037	0.062	-0.163	-0.191	0.021	0.082	0.047	-0.004	-0.101	0.059	1.000	0.052	-0.061
24	0.27136	-0.028	-0.109	-0.022	-0.077	-0.063	0.048	0.010	0.125	0.014	0.010	-0.006	0.011	-0.008	0.052	1.000	0.011
25	0.93063	0.104	0.013	-0.036	-0.010	0.119	-0.032	-0.038	-0.041	0.086	-0.076	-0.072	-0.085	-0.042	-0.061	0.011	1.000
26	0.95481	-0.017	0.004	0.047	0.038	-0.038	0.020	0.049	-0.035	0.141	0.080	-0.289	0.001	-0.163	-0.063	0.008	-0.571
		1.000	-0.071	-0.050	-0.052	-0.039	-0.087	-0.070	-0.070	0.002							
30	0.90764	0.306	0.380	-0.107	0.109	0.052	-0.637	-0.251	-0.080	-0.131	-0.081	-0.012	0.055	-0.120	0.237	-0.114	0.101
		-0.071	1.000	0.119	-0.023	-0.121	0.050	0.216	-0.124	0.033							
31	0.97478	-0.191	0.000	0.023	-0.082	-0.104	-0.167	0.139	0.369	-0.010	0.030	0.015	0.046	-0.038	0.011	-0.009	-0.066
		-0.050	0.119	1.000	-0.120	-0.062	0.513	-0.570	-0.799	0.026							
32	0.93358	0.104	0.009	-0.032	0.025	0.303	0.275	0.066	-0.088	0.034	-0.312	-0.068	-0.084	0.080	-0.014	0.011	0.144
		-0.052	-0.023	-0.120	1.000	-0.134	0.017	-0.119	-0.158	-0.114							
33	0.98465	0.635	0.147	-0.177	0.285	0.667	0.313	-0.594	-0.384	-0.068	0.004	-0.041	0.027	-0.008	0.062	-0.037	0.005
		-0.039	-0.121	-0.062	-0.134	1.000	-0.718	-0.412	-0.188	0.014							
34	0.94315	-0.541	-0.257	0.064	-0.360	-0.583	-0.250	0.546	0.531	-0.012	-0.012	-0.019	-0.034	-0.004	-0.065	0.030	-0.044
		-0.087	0.050	0.513	0.017	-0.718	1.000	0.009	-0.246	-0.033							
35	0.95845	0.013	0.014	-0.176	-0.135	-0.383	-0.263	0.026	-0.033	-0.110	-0.041	-0.100	0.295	-0.075	0.035	-0.003	-0.055
		-0.070	0.216	-0.570	-0.119	-0.412	0.009	1.000	0.628	0.021							
36	0.96737	-0.171	-0.065	0.168	-0.004	-0.215	0.029	0.077	-0.188	-0.028	0.029	0.056	-0.161	-0.018	0.026	0.013	-0.023
		-0.070	-0.124	-0.799	-0.158	-0.188	-0.246	0.628	1.000	0.047							
37	0.82074	-0.008	0.034	0.057	-0.031	-0.171	-0.162	-0.036	0.098	-0.061	-0.041	0.093	0.032	-0.055	0.018	0.005	-0.149
		0.002	0.033	0.026	-0.114	0.014	-0.033	0.021	0.047	1.000							

Of the central values of δ_k's themselves, most are shifted less than one unit of error from the central value of zero. The only quantity that is shifted significantly outside the original systematic error limits is m_c for the combined F_2 and xF_3 fit. The results of the $+1\,\delta(m_c)$ shift from Table 7.12 with the offset from Table 7.14 indicate that $\Lambda_{\overline{\text{MS}}}^{\text{NLO}}$ is shifted by $10\ MeV \times -1.22 = -12\ MeV$ due to m_c in the global systematic fit.

The following tests were made to confirm the results of the global systematic fit. The sensitivity of the fit to the starting values of all the MINUIT fit parameters, including the δ_k's, was tested by randomly setting the starting values of fit to plus or minus two standard error units from the final values found in previous fits. The final values of the fit did not depend on the starting values. The χ^2 variation of each δ_k variable was plotted to plus or minus five units of error from the central values found by the fit, and all were found to be parabolic with the minimum at the final value.

Table 7.18 compares the value of $\Lambda_{\overline{\text{MS}}}^{\text{NLO}}$ from the basic approach to the systematic errors to the results of the global QCD fit. The error on $\Lambda_{\overline{\text{MS}}}^{\text{NLO}}$ from the global systematic fit includes both the statistical and systematic error combined, and so the "systematic" error for the global fit was determined by subtracting in quadrature the statistical error from the basic fit. The Table shows that the global systematic fitting technique substantially reduces the χ^2 of the fit (12 units for the xF_3-only fit and 34 units for the combined F_2 and xF_3 fit). The size of the combined statistical and systematic error is also reduced in half. The value of $\Lambda_{\overline{\text{MS}}}^{\text{NLO}}$ is shifted by $-44\ MeV$ for the combined global systematic F_2 and xF_3 fit; Table 7.14 shows that this is due to larger shifts in the δ_k's in the combined fit compared to the xF_3-only fit.

Table 7.18: Comparison of $\Lambda_{\overline{\mathrm{MS}}}^{\mathrm{NLO}}$ from the basic fit and the global systematic fit. Units are MeV. The "systematic" error from the global fit is derived by subtracting the statistical error in quadrature from the combined error.

	$\Lambda_{\overline{\mathrm{MS}}}^{\mathrm{NLO}}$ from xF_3-only fit			$\Lambda_{\overline{\mathrm{MS}}}^{\mathrm{NLO}}$ from combined F_2 and xF_3 fit		
	Stat and Syst	Combined Error	χ^2/DOF	Stat and Syst	Combined Error	χ^2/DOF
Basic Fit	$387 \pm 42 \pm 93$	336 ± 102	81/82	$381 \pm 24 \pm 51$	346 ± 56	191/164
Global Fit	$381 \pm 41 \pm 34$	381 ± 53	69/82	$337 \pm 21 \pm 19$	337 ± 28	157/164

Overall, the values of $\Lambda_{\overline{\mathrm{MS}}}^{\mathrm{NLO}}$ from the different fits are consistent with one another. There is no reason not to choose the value with the smallest overall error. Therefore, the value of $\Lambda_{\overline{\mathrm{MS}}}^{\mathrm{NLO}}$ reported in this analysis is 337 ± 28 (stat + syst) MeV measured at an average value of $\left\langle Q^2 \right\rangle = 30\ GeV^2$. The exponent η_G of the shape of the gluon distribution for this fit is 4.65 ± 0.68.

As discussed in Chapter 8, the standard for comparing the strong coupling constants from different experiments is to quote $\alpha_S(M_Z^2)$. The coupling parameter Λ is converted to α_S using the relation of Equation 7.4, with corrections made at the quark-mass thresholds according to the prescription in Ref. [Bar96]. Thus the value for $\Lambda_{\overline{\mathrm{MS}}}^{\mathrm{NLO},(4)}$ of 337 ± 28 MeV corresponds to $\alpha_S(M_Z^2) = 0.119 \pm 0.002$. An error of 13 MeV from the higher-twist systematic error corresponds to a shift in $\alpha_S(M_Z^2)$ of ± 0.001. From Refs. [Mar91, Vir92], a conservative scale error of 0.004 is assumed. Therefore, the value of $\alpha_S(M_Z^2)$ reported in this analysis is 0.119 ± 0.002 (stat + syst) ± 0.001 (HT) ± 0.004 (theory).